NASA
Technical
Paper
2134

May 1983

The Wedge Hot-Film Anemometer in Supersonic Flow

John M. Seiner

NASA

25th Anniversary
1958-1983

NASA
Technical
Paper
2134

1983

The Wedge Hot-Film Anemometer in Supersonic Flow

John M. Seiner
Langley Research Center
Hampton, Virginia

NASA
National Aeronautics
and Space Administration

**Scientific and Technical
Information Branch**

SUMMARY

The convective heat transfer properties of a commercial wedge hot-film probe with a 40° semivertex angle are examined to determine its response in transonic and low supersonic flows of high unit Reynolds number (i.e., 20×10^6 to 280×10^6 per meter). The results of the study show that throughout this entire flow regime, the probe response depends on free-stream Mach number and consequently shows a greater sensitivity to velocity than to density fluctuations. The "local linearization method" of Kovásznay and Morkovin is used to derive the wedge probe sensitivities to the various modal fluctuations. To absorb the Mach number dependence, these sensitivities are derived in terms of free-stream Reynolds number rather than stagnation Reynolds number. The dependence of the probe sensitivities on the flow parameters and temperature loading is then examined. This analysis shows that the probe density sensitivity is only weakly dependent on temperature loading. This weak dependence leads to irregular behavior in the solution for the modal fluctuations. A method is recommended to solve for the modal fluctuations to within an arbitrary factor depending on free-stream static pressure fluctuations. Both the frequency response (130 kHz) and the durability of the probe are satisfactory, but the wedge probe exhibits poor yaw directional response at sonic speeds.

INTRODUCTION

This paper examines the convective heat transfer properties of a commercial wedge-shaped hot-film probe in the transonic to low supersonic flow regime. Of particular interest are those supersonic flows associated with the turbulent jet shear layer at high unit Reynolds number (i.e., greater than 10^6 per meter) for which a hot-wire probe has insufficient mechanical strength. This work originates from a need to obtain turbulent flow details with high frequency response for the study of sound generation from shock-free and shock-containing supersonic jets.

Ling and Hubbard (1956) introduced the wedge-shaped hot-film probe as a new device for turbulent flow research. This probe consisted of a thin layer of platinum film fused to a wedge-shaped glass surface. The probe was developed as a means for studying flows for which hot-wire probes would be impractical, such as liquid and high speed supersonic gas flows that require a probe with high mechanical strength. Despite the high frequency response (100 kHz) obtained near sonic velocities by Ling and Hubbard with their probe, the wedge hot-film probe received little attention in high speed applications until the work of Glaznev (1973), who used a commercial version of the wedge probe in a supersonic choked jet airstream.

While Glaznev did not directly specify how the probe voltage signal was interpreted in terms of the physical variables, the paper indicated that the procedure used was the modal analysis method introduced by Kovásznay (1950 and 1953) and Morkovin (1956) for the cylindrical hot-wire probe. Like Glaznev, our primary motivation for using the wedge probe was an interest in obtaining relevant turbulent flow components that could be used to improve understanding of the physical mechanisms associated with noise production by high speed jet flows. However, initial calibration tests in the Langley Jet-Noise Laboratory with a commercial hot-film wedge probe, similar to Glaznev's, demonstrated that its response in supersonic flow was significantly different from that observed for cylindrical type sensors. Thus, this

paper reports the results of a study whose purpose was to examine the supersonic properties of wedge-shaped hot-film anemometry probes and to provide a means for interpreting their voltage signal in terms of the physical variables.

The supersonic properties of the wedge hot-film probe were established by positioning a wedge probe at the exit of a supersonic nozzle. During the course of the investigation, three nozzles were used with nominal exit Mach numbers of 1.0, 1.5, and 2.0. The results of these calibrations demonstrated that the wedge probe response is Mach number dependent, but that this dependence can be absorbed when the response is analyzed in terms of a Reynolds number based on the free-stream static temperature. Cylindrical hot-wire probes are analyzed in terms of a Reynolds number based on stagnation temperature, and as previously shown by Laufer and McClellan (1956) their response becomes independent of free-stream Mach number above 1.3.

This paper provides details of the calibration method used to determine the response of the wedge probe in the high unit Reynolds number range of 20×10^6 to 280×10^6 per meter. In addition, sensitivity equations are derived which describe the observed behavior of the probe. The derived sensitivity coefficients are examined to determine their dependence on the flow parameters (i.e., Mach and Reynolds numbers) and temperature loading. Based on these results, a procedure is recommended which can be used to interpret the measured bridge voltage fluctuations in terms of the fluctuating flow variables. The wedge probe behavior is also compared with the response of cylindrical hot-film sensors which were also examined using the same calibration method. In this way, a fair estimation of the capabilities of the calibration method could be related to prior research results, and an estimation of the conduction end loss could be examined. The directional response of each probe type is also briefly examined to establish capabilities of each probe for Reynolds stress measurements using dual sensor configurations. A typical application of the wedge probe to supersonic turbulent flow measurements can be found in Seiner and Yu (1981) and Seiner, McLaughlin, and Liu (1982).

SYMBOLS

A_{ij} probe transformation matrix (eq. (26))

A^{-1} inverse matrix (eq. (27))

$A(\theta)$ probe sensitivity to free-stream Reynolds number (eq. (28))

$B(\theta)$ wedge hot-film probe intercept (eq. (28))

c sound speed

D probe diameter or wedge thickness (fig. 1)

E_b, e' mean and fluctuating bridge voltage

E_i measured probe voltage array (eq. (26))

e'_c, e'_p pseudo voltages (eqs. (40) and (41))

f function defined by equation (30)

g function defined by equation (32)

h_c convective heat transfer coefficient

I_p probe current

k directional probe response parameter (eq. (44))

k_o thermal conductivity of air

L length of film plating on cylinder or wedge

M Mach number

m_o $d(\ln \mu_o)/d(\ln T_o)$

Nu_o Nusselt modulus, $h_c D/k_o$

n_o $d(\ln k_o)/d(\ln T_o)$

P,p' mean and fluctuating pressure

Q_c, Q_k convective and conductive heat transfer rate

R_a probe resistance at 293.15 K

Re Reynolds number, $\rho UD/\mu$

R_L, R_p, R_r leads, probe, and recovery resistance

S_ρ, S_u, S_T, S_p probe sensitivity to density, velocity, temperature, and pressure

T_o, T_o' mean and fluctuating stagnation temperatures

T_p, T_r, T_∞ probe, recovery, and free-stream temperatures

U,u' mean and fluctuating free-stream velocity

X_j unknown variable array (eq. (26))

α film resistance temperature coefficient

α_o coefficient defined by equation (22)

α_1 coefficient defined by equation (23)

γ ratio of specific heats

ε $= Q_k/(Q_k + Q_c)$

η temperature recovery ratio, T_r/T_o

θ overheating parameter, T_p/T_o

μ absolute viscosity

ρ, ρ' mean and fluctuating free-stream density

τ temperature overheat (eq. (4))

τ_{wr} temperature loading (eq. (24))

ϕ probe yaw angle

Subscripts:

a ambient value

o stagnation condition

ref reference quantity

∞ free-stream value

A bar over a symbol denotes time average.

HOT-FILM PROBES AND CALIBRATION PROCEDURE

Four hot-film probes (three wedge shaped and one cylindrical) were used in this study. Schematic diagrams of these commercial probes are shown in figures 1 and 2. Table I lists several relevant properties of these probes.

All the probes listed in table I have a 1000-Å layer of nickel sputtered on a glass substrate. The thin nickel film serves as the heat source medium for heat transfer to the fluid medium, analogous to the fine wire of a hot-wire probe. Since these probes were designed for use in liquid flows, they have a thin outer protective layer of quartz deposited over the nickel to prevent electrical shorts. In high speed gas flows, this layer protects the nickel against abrasive contaminants which can lead to early probe burnout. The probes in table I have a 2.0-μm outer protective quartz coating except for probe W which has a 0.5-μm coating. Probe frequency response is inversely proportional to the thickness of the protective quartz coating.

The supersonic properties of the wedge probes were established by locating a probe at the exits of different supersonic nozzles where the flow is essentially uniform and turbulence free. Three supersonic nozzles with design exit Mach numbers of 1.0, 1.5, and 2.0 were operated in and around their design point. These nozzles have respective exit diameters of 3.962, 4.268, and 4.989 cm. For a given supersonic nozzle and constant supply temperature, there is a nozzle pressure ratio range around the design point where the jet exit velocity remains constant. In this range, a linear variation of the nozzle pressure ratio produces a proportionally linear variation in the jet exit density. This is true for all nozzle pressure ratios producing underexpanded flow or producing overexpanded flows without a normal shock. This nozzle exit condition is summarized in figure 3, which shows the measured variation of the mean mass flux at the exit for each of the three nozzles. These data are normalized by the mean mass flux $(\rho U)_{ref}$ obtained when operating each nozzle at its design point.

The data of figure 3 bracket the entire test range for the hot-film probe calibrations. The data were established by measurement of the exit stagnation and static pressure and the supply stagnation temperature. The small region in figure 3 showing a nonlinear variation of mass flux with pressure ratio was obtained by operating the Mach 1.0 nozzle at subcritical pressure ratios. Thus in this subsonic range, probe

calibrations were obtained with a constant jet exit density and a variable exit velocity. The data of figure 3 show that with this method of calibration, it is possible to obtain a 10 to 1 variation of the parameters for probe calibration.

The response of anemometry probes is commonly expressed in terms of the non-dimensional Nusselt modulus $Nu_o = h_c D/k_o$, where h_c represents the convective heat transfer coefficient and k_o the gas thermal conductivity at stagnation conditions. The Nusselt modulus is a measure of the heat transferred by the probe to the surrounding fluid medium by convection. For probes that have a small aspect ratio, a significant amount of heat is also transferred by conduction to supporting members. Using the end conduction loss corrections of Lord (1974), Ho, McLaughlin, and Troutt (1978) have shown that in low Reynolds number supersonic flows, the sensor response is often dominated by this component at low probe temperature overheats (i.e., $\theta = T_p/T_o$ near unity). The heat balance equation for constant-temperature anemometer probes is given by

$$I_p^2 R_p = Q_c + Q_k \tag{1}$$

which simply expresses that ohmic heating in the absence of radiative heat losses is balanced by convective Q_c and conductive Q_k heat transfer. Since most anemometry sensors are rarely operated above 300°C, heat loss due to radiation is negligible.

The present investigation involves the study of the wedge-shaped hot-film anemometer in high Reynolds number supersonic flows. In this flow regime, as shown in the next section, the conductive heat transfer contribution is considerably smaller than that due to convection. Under these conditions, probe end loss corrections are small and ohmic heating is balanced principally by the convective heat transfer mode. In terms of the Nusselt modulus Nu_o and temperature recovery ratio ($\eta = T_r/T_o$), the ohmic heating is given by

$$I_p^2 R_p = Q_c = aLk_o(T_p - \eta T_o)Nu_o \tag{2}$$

where the parameter a is equal to 2 for a wedge probe and to π for a cylindrical probe. In equation (2), T_p and T_o refer respectively to the probe temperature and fluid stagnation temperature. From equation (2), the Nusselt modulus can be expressed in terms of the probe electrical quantities as

$$Nu_o = \frac{\alpha E_b^2}{ak_o L} \frac{\tau + 1}{\tau} \frac{R_r}{\left[R_r(\tau + 1) + R_L + 50\right]^2} \tag{3}$$

where the temperature overheat, probe resistance, and probe current (for a 50-Ω, 1-to-1 bridge) are given by

$$\tau = \frac{R_p - R_r}{R_r} = \alpha(T_p - \eta T_o) \tag{4}$$

$$R_p = R_r[1 + \alpha(T_p - T_r)] \tag{5}$$

$$I_p = \frac{E_b}{R_r(\tau + 1) + R_L + 50} \tag{6}$$

In equation (3), E_b, R_r, and R_L refer respectively to the measured anemometer bridge voltage, the probe recovery resistance, and the leads resistance. The parameter α is the film resistance temperature coefficient. The Nusselt modulus and the fluid thermal conductivity in equation (3) are referenced to the stagnation temperature. All heat transfer data presented in this paper are based on the Nusselt modulus as determined from equation (3).

MEASURED HOT-FILM PROBE RESPONSE

When conduction end losses are negligible, Kovásznay (1953) and Morkovin (1956) have shown that the heat transfer from a hot wire depends dimensionally on the flow parameters as follows:

$$\left.\begin{aligned} Nu_o &= Nu_o(M, Re_o, \theta) \\ \eta &= \eta(M, Re_o) \end{aligned}\right\} \tag{7}$$

where $\theta = T_p/T_o$ is the overheating parameter and M is the free-stream Mach number.

On the basis of this analysis, probe calibration results are customarily analyzed in terms of a Reynolds number based on stagnation temperature conditions (i.e., $Re_o = \rho UD/\mu_o$). As can be observed in Figure 4, the response of the cylindrical hot-film sensor, probe 3, compares favorably on this basis with the asymptotic empirical heat transfer correlation derived by Behrens (1971) for hot-wire probes with conduction end loss correction. As previously demonstrated by Laufer and McClellan (1956) for lower cylindrical probe Reynolds numbers, this comparison shows that the cylindrical probe response does not depend on Mach number when $M > 1.3$. The results also show that at high probe Reynolds numbers, end conduction losses are small in view of the agreement with Behren's asymptotic curve. This view is also supported by the heat conduction estimate of the appendix. This estimate shows that this mode accounts for no more than 7.5 percent of the total heat transferred and that its influence diminishes with increasing probe Reynolds numbers. These results agree with the data shown in figure 4 and suggest that conduction end losses can be assumed small for the wedge probe because of similarities in the thermal properties of the materials used in its construction.

Typical results for the wedge hot-film probe are shown in figure 5 for exit Mach numbers of 1.00, 1.41, and 1.99. Unlike the behavior of the cylindrical probe, these data definitely depend on free-stream Mach number when correlated with the stagnation Reynolds number. Although these data are for probe Z of table I, all other wedge probes exhibited a similar behavior in terms of the stagnation Reynolds number. This

behavior can be better understood by examining the dependence of the Nusselt modulus directly on the physical variables.

From the same data set as in figure 5, the Nusselt modulus is correlated in figure 6 with the free-stream density ratio $(\rho/\rho_a)^{1/2}$. Here ρ_a represents the ambient density to which the supersonic jet exhausts. In this figure, the free-stream velocity appears as a parameter and is a constant for each of the three free-stream Mach numbers, since the supply stagnation temperature is constant. This particular data correlation represents the method by which the data are actually obtained from each supersonic nozzle. It is apparent from figure 6 that the Nusselt modulus correlates well with $(\rho/\rho_a)^{1/2}$ when the free-stream velocity is held constant. If the wedge probe had the same sensitivity to density as to velocity, the data of figure 6 would correlate with $(\rho U)^{1/2}$. However, as shown in figure 7, the Nusselt modulus for the three Mach numbers correlates instead with $\rho^{0.5}U^{0.765}$. This behavior clearly suggests that the wedge hot-film probe exhibits greater sensitivity to velocity than to density over the entire test range of this study. The significance of this particular exponent of velocity is demonstrated below.

The Nusselt modulus represents a measure of the similarity between the hydrodynamic and thermal boundary layers by virtue of the dependence of the convective heat transfer coefficient on the flow variables. It is of interest to note the empirical relationship between the absolute gas viscosity and temperature as given by

$$\mu_\infty/\mu_o = (T_\infty/T_o)^{m_o} \tag{8}$$

Morkovin (1956) gives a value for m_o of 0.765 for air temperatures between 270 K and 350 K. Since the data of figure 7 correlate well with the same exponent for velocity, a correlation of the wedge probe data with free-stream Reynolds number is suggested as a means for incorporating the apparent Mach number effect:

$$Re_\infty = Re_o(\mu_o/\mu_\infty) = Re_o(T_o/T_\infty)^{m_o} \tag{9}$$

In equation (9), the relationship between the Reynolds numbers based on the free-stream static (Re_∞) and stagnation (Re_o) temperatures is modified by a term which depends on the free-stream velocity outside the thermal boundary layer of the wedge probe surface.

In figure 8, the wedge film calibration data of figure 5 for probe Z, are presented in terms of free-stream Reynolds number. It is apparent that this parameter correctly absorbs the Mach number dependence in the calibration data, and therefore represents the appropriate manner by which to view these data. Figures 8(b) and 8(c), for probes Y and W, demonstrate similar behavior with the free-stream Reynolds number. The least square fits to the data in figures 8(a) through 8(c) show small differences in operating performance. On this basis, the heat transfer from a wedge-shaped hot-film probe would depend dimensionally on the flow parameters as follows:

$$\left.\begin{aligned} Nu_o &= Nu_o(Re_\infty, \theta) \\ \eta &= \eta(M, Re_\infty) \end{aligned}\right\} \tag{10}$$

in contrast to the parametric dependence for cylindrical probes expressed by equation (7). In the following section, this parametric dependency on the flow variables is used to derive the sensitivity coefficients for the wedge film probe, which are similar to those derived by Morkovin for the cylindrical sensor.

ANALYSIS OF EXPERIMENTAL RESULTS

Wedge Hot-Film Sensitivity Coefficients

To obtain the fluctuating flow variables, variations in the anemometer output must be expressed in terms of the flow variable fluctuations. On the basis of Morkovin's analysis for cylindrical sensors, the fluctuating anemometer bridge voltage is customarily expressed in terms of density ρ, velocity U, and stagnation temperature T_o. By using equations (2) and (6), and noting that $d\{\ln[R_p/(R_p + R_L + 50)^2]\} = 0$ for constant-temperature operation, the bridge voltage variations can be expressed in terms of the fluctuating flow variables as

$$d(\ln E_b) \approx \frac{e'}{E_b} = \frac{1}{2} d(\ln Q_c) \tag{11}$$

since $d(\ln E_b) \approx \Delta E_b/E_b$. The approximation in equation (11) is due to Kovásznay (1953) and Morkovin (1956) and is known formally as "the local linearization method." As such, the approximation is only valid for those points in a flow where the local turbulence intensity level is not high (i.e., less than 20 percent). The logarithmic derivative of the convective heat transfer rate Q_c can be determined from equation (2) as

$$\begin{aligned}\frac{1}{2} d(\ln Q_c) = {} & \frac{1}{2}\left[\frac{\partial(\ln Nu_o)}{\partial(\ln Re_\infty)} - \frac{\eta}{\theta - \eta}\frac{\partial(\ln \eta)}{\partial(\ln Re_\infty)}\right] d(\ln Re_\infty) \\ & - \frac{1}{2}\left[\frac{\eta}{\theta - \eta}\frac{\partial(\ln \eta)}{\partial(\ln M)}\right] d(\ln M) \\ & + \frac{1}{2}\left[n_o - \frac{\partial(\ln Nu_o)}{\partial(\ln \theta)} - \frac{\eta}{\theta - \eta}\right] d(\ln T_o) \\ & + \frac{1}{2}\left[\frac{\partial(\ln Nu_o)}{\partial(\ln \theta)} + \frac{\theta}{\theta - \eta}\right] d(\ln T_p)\end{aligned} \tag{12}$$

where $d(\ln \theta) = d(\ln T_p) - d(\ln T_o)$ and

$$n_o = \frac{d(\ln k_o)}{d(\ln T_o)} \tag{13}$$

Morkovin gives a value of 0.885 for n_o for air in the temperature range from 270 K to 350 K. For constant-temperature anemometry, $d(\ln T_p) = 0$ by definition and is not considered further. Equation (12) can be put in a form compatible with Morkovin's cylindrical probe results by considering the relation $d(\ln \mu_\infty) = m_o\, d(\ln T_\infty)$, which follows from equation (8), along with the following useful relations:

$$d(\ln Re_\infty) = d(\ln \rho) + d(\ln U) - m_o\, d(\ln T_\infty) \tag{14}$$

$$d(\ln T_\infty) = d(\ln T_o) - \frac{(\gamma - 1)M^2}{1 + \frac{\gamma - 1}{2} M^2}\, d(\ln M) \tag{15}$$

$$d(\ln c_\infty) = d(\ln c_o) - \frac{\frac{\gamma - 1}{2} M^2}{1 + \frac{\gamma - 1}{2} M^2}\, d(\ln M) \tag{16}$$

$$d(\ln M) = d\left(\ln \frac{U}{c_\infty}\right) = \left(1 + \frac{\gamma - 1}{2} M^2\right)\left[d(\ln U) - \frac{1}{2}\, d(\ln T_o)\right] \tag{17}$$

Substitution of the above relations in equation (12) produces the following heat balance equation for balanced constant-temperature wedge probe anemometry:

$$\frac{e'}{E_b} = S_\rho \frac{\rho'}{\rho} + S_u \frac{u'}{U} - S_T \frac{T_o'}{T_o} \tag{18}$$

where the sensitivity coefficients are given by

$$S_\rho = \frac{1}{2}\left[\frac{\partial(\ln Nu_o)}{\partial(\ln Re_\infty)} - \frac{1}{\tau_{wr}} \frac{\partial(\ln \eta)}{\partial(\ln Re_\infty)}\right] \tag{19}$$

$$S_u = \frac{1}{2}\left\{\alpha_1\left[\frac{\partial(\ln Nu_o)}{\partial(\ln Re_\infty)} - \frac{1}{\tau_{wr}} \frac{\partial(\ln \eta)}{\partial(\ln Re_\infty)}\right] - \frac{1}{\alpha_o \tau_{wr}} \frac{\partial(\ln \eta)}{\partial(\ln M)}\right\} \tag{20}$$

$$S_T = \frac{1}{2}\left\{\frac{m_o}{\alpha_o}\left[\frac{\partial(\ln Nu_o)}{\partial(\ln Re_\infty)} + \frac{1}{\tau_{wr}}\frac{\partial(\ln \eta)}{\partial(\ln Re_\infty)}\right] + \frac{1}{\tau_{wr}} + \frac{\partial(\ln Nu_o)}{\partial(\ln \theta)}\right.$$

$$\left. - \frac{1}{2\alpha_o \tau_{wr}}\frac{\partial(\ln \eta)}{\partial(\ln M)} - n_o\right\} \tag{21}$$

and the coefficients α_o, α_1, and τ_{wr} by

$$\alpha_o = \left(1 + \frac{\gamma - 1}{2} M^2\right)^{-1} \tag{22}$$

$$\alpha_1 = 1 + m_o(\gamma - 1)M^2 \tag{23}$$

$$\tau_{wr} = \frac{\theta - \eta}{\eta} \tag{24}$$

In the next section the fluctuating flow variables are determined from solution of equation (18).

Determination of Fluctuating Flow Variables

The flow fluctuation variables ρ', u', and T_o' are related to the measured anemometer bridge voltage fluctuation e' through the locally linearized equation (18), which is valid only for small flow fluctuations. As previously shown by Kovásznay (1953) and Morkovin (1956), the flow fluctuations can be determined from equation (18) through variation of the single adjustable parameter τ_{wr} that appears in sensitivity equations (19), (20), and (21). Since the probe can be operated only at a single value of τ_{wr} at one time, only the mean and mean square fluctuating anemometer bridge voltages can be considered relevant. Thus, the flow fluctuation variables are actually obtained from the square and average of equation (18) as follows:

$$\frac{\overline{e'^2}}{E_b^2} = S_\rho^2 \frac{\overline{\rho'^2}}{\rho^2} + S_u^2 \frac{\overline{u'^2}}{U^2} + S_T^2 \frac{\overline{T_o'^2}}{T_o^2} + 2S_\rho S_u R_{\rho u} - 2S_\rho S_T R_{\rho T} - 2S_u S_T R_{uT} \tag{25}$$

where the correlation coefficients are given by $R_{\rho u} = \overline{\rho' u'}/\rho U$, $R_{\rho T} = \overline{\rho' T_o'}/\rho T_o$, and $R_{uT} = \overline{u' T_o'}/U T_o$.

Equation (25) contains six unknowns, the mean square flow fluctuation variables ρ'^2, u'^2, and $T_o'^2$ and their mutual correlations $R_{\rho u}$, $R_{\rho T}$, and R_{uT}. Solution for these quantities requires that the probe be operated at a minimum of six probe temperature overheats for constant mean free-stream conditions and that the mean

free-stream Mach number be determined by an independent measurement to satisfy auxiliary equations (22) and (23) for α_o and α_1. The resulting system of six linear algebraic equations based on equation (25) can be written in matrix form as

$$A_{ij}X_j = E_i \tag{26}$$

where A_{ij} is a 6 × 6 matrix containing the sensitivity coefficient factors of equation (25), X_j is a 1 × 6 matrix containing the six unknown variables, and E_i is a 1 × 6 matrix containing the six measured voltage ratios $\overline{e'^2}/E_b^2$. The solution for the flow variables can then be determined from equation (26) by solving for the inverse matrix of A_{ij} as shown by

$$X_j = \frac{A_{ji}}{|A|} = A^{-1}E_i \tag{27}$$

where $|A|$ denotes the determinant and A^{-1} the inverse matrix of A_{ij}.

Horstman and Rose (1977) reported that the A_{ij} matrix is nearly singular for cylindrical probes. In the analysis that follows, the matrix A_{ij} for the wedge probe is found to behave similarly. To demonstrate this behavior, analytical expressions are developed for the various terms that appear in sensitivity equations (19), (20), and (21). In the next several sections, the variation of the wedge probe sensitivity coefficients is related to the flow parameters (i.e., M and Re_∞) and to the temperature loading τ_{wr}.

Variation of Wedge Probe Sensitivity Terms With Flow Parameters

In this section, the various terms appearing in the sensitivity equations for S_ρ, S_u, and S_T are analyzed with respect to their functional dependence on and relative variation with the flow parameters. The complete calibration data file for probe Z is used for this purpose. The following analysis shows that relative to other terms, the dependence of recovery temperature ratio on free-stream Reynolds number (i.e., $\partial(\ln \eta)/\partial(\ln Re_\infty)$) can be considered negligible, but its dependence on free-stream Mach number should in general be retained. In addition, the dependence of the Nusselt modulus on the overheating parameter θ is found to be significant and must always be retained.

In figure 9, the dependence of η on free-stream Reynolds number is shown for free-stream Mach numbers of 1.00, 1.41, and 1.99. For constant free-stream Mach number, η appears to be independent of the free-stream Reynolds number. The variation that does occur for each free-stream Mach number falls within the accuracy of the temperature gauge (±0.1°C or ±0.4 percent of reading) used to measure the stagnation temperature T_o. This can be observed from the data scatter for those points near the same free-stream Reynolds number. This scatter primarily occurs in the sonic data at low Reynolds numbers. The results in figure 9 are consistent with those obtained by Laufer and McClellan (1956) for cylindrical type sensors operating with stagnation Reynolds numbers above 40.

The data in figure 9 do indicate, however, that the temperature recovery ratio for the wedge probe depends on Mach number. In Figure 10, this dependence is examined by using the average values of η for each test Mach number, including the subsonic Mach numbers of 0.50 and 0.90. These data are shown by the open round symbols. A second order least square curve is fitted to these data to enable estimation of the logarithmic derivative variation of η with Mach number. The least square coefficients obtained are included in figure 10. From this least square representation, the logarithmic derivative variation of η with Mach number shown in figure 11 is obtained.

As can be observed in figure 11, the general trend of the resulting variation for the wedge probe is similar to that obtained by Morkovin (1956) for cylindrical sensors with several notable exceptions. The wedge probe variation is more gradual, the peak magnitude is much less, and the peak location occurs at a higher Mach number. The change in the peak location with Mach number can be partially explained by the behavior associated with the probe body shocks; a more slender wedge probe than that of figure 1 would produce a peak at even a higher Mach number. The relative importance of the term $-\partial(\ln \eta)/\partial(\ln M)$ associated with the wedge probe in figure 11 cannot be determined until the dependence of the Nusselt modulus on the temperature overheating parameter θ is examined.

The dependence of the Nusselt modulus on free-stream Reynolds number in figures 8(a) through 8(c) is shown for one temperature overheat condition. Figure 12 shows how the wedge probe response depends on the temperature overheating parameter $\theta = T_p/T_o$, which from equation (4) is related to the temperature overheat τ by $\theta = (\alpha T_o)^{-1}\tau + \eta$. In figure 12, the probe Z data obtained for all Mach numbers examined (i.e., $0.5 \leq M \leq 2.0$) are least squares fitted for each of the three temperature overheats used in this study. These least square coefficients, A and B, are tabulated in figure 12. The data show that the Nusselt modulus decreases with increasing temperature overheating at a constant free-stream Reynolds number and suggest the following relationship to account for the dependence on temperature overheat and Reynolds number:

$$Nu_o(Re_\infty, \theta) = A(\theta)\ (Re_\infty)^{1/2} + B(\theta) \tag{28}$$

From equation (28), the logarithmic derivative of the Nusselt modulus with respect to free-stream Reynolds number at a constant temperature overheat is given by

$$\frac{\partial(\ln Nu_o)}{\partial(\ln Re_\infty)} = \frac{1}{2}\left[1 - \frac{B(\theta)}{Nu_o}\right] \tag{29}$$

With equation (29), the functional dependence of η on Mach number can be investigated as it appears, for example, in sensitivity equation (20) for S_u. The relevant ratio to be considered is

$$f(M,Re_\infty,\theta) = -\frac{\partial(\ln \eta)/\partial(\ln M)}{\alpha_o \alpha_1 \tau_{wr}\, \partial(\ln Nu_o)/\partial(\ln Re_\infty)} \tag{30}$$

where by previous considerations the term $\partial(\ln \eta)/\partial(\ln Re_\infty)$ can be neglected. The function $f(M,Re_\infty,\theta)$ is plotted in figure 13 for three temperature loadings that are pertinent to the wedge probe operation. A constant free-stream Mach number of 1.25 was selected because this value maximizes the term $\partial(\ln \eta)/\partial(\ln M)$, as shown in figure 11. It is apparent from figure 13 that the dependence of η on Mach number should not in general be neglected, particularly when using low values of wedge probe temperature overheat at free-stream Mach numbers near 1.25.

It is now possible to demonstrate an important functional difference between wedge and cylindrical probes, which has an important influence on the solution for the fluctuating flow variables in equation (18). With the dependence of η on Reynolds number again neglected in equations (19) and (20), equations (28) and (29) and the results in figure 11 can be used to estimate the velocity-to-density sensitivity ratio S_u/S_ρ for any given free-stream Mach and Reynolds numbers. This computed ratio is shown in figure 14 as a function of Mach number for a constant free-stream Reynolds number of 20000 and three temperature loadings. The results in figure 14 only weakly depend on the free-stream Reynolds number, and the $Re_\infty = 20000$ was selected because it bisects the range of the current data.

As can be observed in figure 14, the wedge probe sensitivities to velocity and to density are unequal except at one Mach number that depends on the probe temperature loading. In contrast to this behavior, both Laufer and McClellan (1956) and Horstman and Rose (1977) have shown that a cylindrical sensor has an equal sensitivity to velocity and to density in the Mach number range above 1.3. This difference in behavior is entirely attributed to the behavior of probe body shocks; for a cylinder, the shock is essentially normal near the body producing subsonic flow, and for the wedge, the shock is oblique producing supersonic flow.

The computed results above $M = 2.0$ in figure 14 should be interpreted cautiously, since the wedge probe was not examined above this Mach number. The separation of this sensitivity ratio with temperature loading above $M = 2.5$ is strongly influenced by the estimated behavior of the temperature recovery ratio η with Mach number shown in figure 11. It is entirely possible, for example, that η could become independent of Mach number beyond $M = 2.0$. Then, S_u/S_ρ would become independent of temperature loading and monotonically increase with Mach number, as shown by the solid curve in figure 14 for which $S_u/S_\rho = \alpha_1$. Determination of the dependence of η on Mach numbers greater than 2.0 represents an important area for further research on the wedge probe.

To evaluate other sensitivity ratios involving the temperature sensitivity S_T given by equation (21), the dependence of the Nusselt modulus on temperature overheat must be examined more explicitly. Thus, the variation of the logarithmic derivative $\partial(\ln Nu_o)/\partial(\ln \theta)$ is considered next.

A typical variation of the Nusselt modulus with θ is shown in figure 15 for the free-stream Mach number of 1.99. In this figure, the free-stream Reynolds number appears as a parameter, and as expected from the data in figure 12, it accounts for the largest variation in the data. It is evident that an increase in the free-stream Reynolds number is accompanied by an increase in the dependence of Nusselt modulus on θ.

The relative importance of $\partial(\ln Nu_o)/\partial(\ln \theta)$ appearing in sensitivity equation (21) for S_T can be gauged by taking the logarithmic derivative of equation (28) with respect to θ at a constant free-stream Reynolds number as follows:

$$\frac{\partial(\ln Nu_o)}{\partial(\ln \theta)} = \frac{\theta}{Nu_o}\left[(Re_\infty)^{1/2}\frac{\partial A(\theta)}{\partial \theta} + \frac{\partial B(\theta)}{\partial \theta}\right] \tag{31}$$

Equation (31) makes use of the empirical coefficients $A(\theta)$ and $B(\theta)$ and explicitly displays the dependence on free-stream Reynolds number. The Nu_o term appearing in equation (31) can be calculated from equation (28). Figure 16 shows the results obtained from equation (31) to estimate the term $\partial(\ln Nu_o)/\partial(\ln \theta)$. Only a few free-stream Reynolds numbers are shown, but these bracket the range in this investigation. The data obtained at these selected Reynolds and Mach numbers are shown by the plotted symbols. They are determined by direct evaluation of the logarithmic derivative from relevant data such as those shown in figure 15. As can be observed in figure 16, equation (31) provides a reasonable estimate for the variation of the logarithmic derivative of the Nusselt modulus with temperature overheat for the entire Mach number and Reynolds number ranges investigated.

By using equation (31), the relative dependence of the Nusselt modulus on temperature overheat can be estimated in the sensitivity equation (21) for S_T. The relevant ratio to be considered is

$$g(M,Re_\infty,\theta) = \frac{\dfrac{\partial(\ln Nu_o)}{\partial(\ln \theta)}}{\dfrac{m_o}{\alpha_o}\dfrac{\partial(\ln Nu_o)}{\partial(\ln Re_\infty)} + \dfrac{1}{\tau_{wr}} - \dfrac{1}{2\alpha_o \tau_{wr}}\dfrac{\partial(\ln \eta)}{\partial(\ln M)} - n_o} \tag{32}$$

where again the term $\partial(\ln \eta)/\partial(\ln Re_\infty)$ is neglected. The function $g(M,Re_\infty,\theta)$ is plotted in figure 17 for the same three temperature loadings used in figure 13. As can be observed in figure 17, the logarithmic derivative of the Nusselt modulus with respect to temperature overheat is of increasing importance as temperature overheat increases, and its relative contribution to the evaluation of S_T cannot be neglected. The selection of a free-stream Mach number of 1.25 in equation (29) produces a minimum absolute value with respect to Mach number for the function $g(M,Re_\infty,\theta)$. This can be seen by recalling figure 11 for the dependence of η on Mach number. Thus, the results of figure 17 represent a minimum contribution for the term $\partial(\ln Nu_o)/\partial(\ln \theta)$.

To summarize the results of this section, the above analysis has shown that the wedge probe dependence of η on Reynolds number can be neglected, but the dependence of η on Mach number should be retained. The dependence of the Nusselt modulus on temperature overheat was found to be significant and must always be retained. The wedge probe sensitivities to velocity and to density were found to be unequal for the entire Mach number range examined (i.e., $0.5 \leq M \leq 2$).

The above results pertain to wedge probe Z. Even though the other wedge probes show no significant deviation from these results, small differences in probe behavior do occur. To minimize these differences in solving for the inverse matrix A^{-1} of equation (27), each probe must be independently calibrated with respect to its particular dependence on $Nu_o(Re_\infty, \theta)$ and $\eta(M)$.

Variation of Wedge Probe Sensitivities With Temperature Loading

In the preceding section, various terms in the sensitivity equations for S_ρ, S_u, and S_T were analyzed using the complete probe Z calibration data file. This analysis provided the means to numerically estimate the three modal sensitivities for any given free-stream Mach and Reynolds numbers. In this section, these sensitivities are examined to determine their relative variation with respect to probe film temperature loading, as expressed by the variable τ_{wr} defined by equation (24).

The variation of the temperature loading provides the mechanism for solving equation (18) for the flow fluctuation variables ρ', u', and T_o'. The accuracy of the solution to equation (18) is integrally related to the variation of the sensitivity ratios S_T/S_u, S_T/S_ρ, and S_u/S_ρ with temperature loading. When there is a small variation of any of these sensitivity ratios with temperature loading, then the transformation matrix A_{ij} of equation (26) is nearly singular.

Figure 18 shows the estimated variation of the sensitivity ratio S_T/S_u with temperature loading for several free-stream Mach numbers that bracket the range of this investigation (i.e., $0.5 \leq M \leq 2$). Figure 18(a) refers to results when $Re_\infty = 2500$, and figure 18(b) when $Re_\infty = 35000$. The estimated sensitivity ratio is obtained by using the analysis of the preceding section to determine the appropriate logarithmic derivatives. The computed results in figure 18 show that the ratio S_T/S_u varies nonlinearly with temperature loading, the most rapid variation occurring at lower values of τ_{wr}. The calculated data appear functionally similar, the magnitude of S_T/S_u being modified by a change in free-stream Mach or Reynolds number.

The variation of the sensitivity ratio S_T/S_ρ with the temperature loading is similar as shown in figure 19. Figure 19(a) shows that this ratio depends only weakly on free-stream Mach number. Figure 19(b) shows the dependence of this ratio with free-stream Reynolds number as a parameter at a free-stream Mach number of 1.25. In contrast to the variation of either S_T/S_u or S_T/S_ρ with temperature loading, the S_u/S_ρ ratio depends much less on temperature loading, as shown in figure 20. Figure 20(a) shows this dependence at $Re_\infty = 2500$. Figure 20(b) indicates that increasing Reynolds number further weakens the dependence of the ratio S_u/S_ρ on temperature loading.

The relatively weak dependence of S_u/S_ρ on temperature loading requires further investigation into the individual variation of the S_u and S_ρ sensitivities with the parameter τ_{wr}. Figures 21(a) and 21(b) respectively show the dependence of S_u and S_ρ on τ_{wr} for several free-stream Reynolds numbers at a constant

free-stream Mach number of 1.25. Clearly, the wedge probe sensitivity to density S_ρ is for all practical purposes independent of the parameter τ_{wr}. Inclusion of this sensitivity in the transformation matrix A_{ij} of equation (26) produces a nearly singular matrix. Actual computations with this estimated density sensitivity produced irregular results for the resulting inverse matrix A^{-1} of equation (27). These results strongly suggest that, as shown by figure 21(b), the density sensitivity be treated as independent of τ_{wr}. In the next section, the above consideration is implemented to demonstrate how one can interpret the wedge probe response.

RECOMMENDED METHOD OF SOLUTION FOR FLUCTUATING FLOW VARIABLES

On the basis of the results in the preceding section concerning the relative independence of the sensitivity S_ρ to temperature loading, it is clear that given the ±0.4-percent accuracy of the current measurements, equation (18) cannot be solved for the three independent modal fluctuations. However, by assuming that the sensitivity S_ρ is independent of τ_{wr}, as supported by figure 21(b), equation (18) can be solved for both velocity and temperature fluctuations to within an arbitrary factor. Two possibilities arise at this point.

Either the arbitrary factor can be left related to density fluctuations or it can be related to static pressure fluctuations. With supporting optical measurements, the density mode would be preferred; however, with supporting probe measurements, the pressure mode would be preferred with the following advantages. Solution of auxiliary equations (22) and (23) already requires an independent measure of the mean static and total pressures to solve for the local free-stream Mach number. The static pressure measurements can be extended to include the fluctuating part. Additionally, in a free supersonic mixing layer, particularly a heated one, pressure fluctuations are always smaller than density fluctuations because of the high modal correlation between density and temperature. Thus, because of the higher sensitivities to velocity and temperature inherent to the wedge probe operation, as demonstrated by figures 19 and 20, the arbitrary factor related to pressure can be assumed small and can often be neglected to yield a first order solution to equation (18). In this paper, the arbitrary factor is related to pressure fluctuations to take advantage of this feature as shown below.

For a perfect gas, density fluctuations are related to pressure and temperature fluctuations by

$$d(\ln \rho) = d(\ln P) - d(\ln T_o) \tag{33}$$

Substituting equation (33) into equation (14) for $d(\ln \rho)$ and using equations (15), (16), and (17), results in the following alternate expression for the logarithmic variation of the free-stream Reynolds number:

$$d(\ln Re_\infty) = d(\ln P) + \alpha_1\, d(\ln U) - \left(1 + \frac{m_o}{\alpha_o}\right) d(\ln T_o) \tag{34}$$

With equation (34) substituted in equation (12) instead of equation (14) for $d(\ln Re_\infty)$, equation (18) can be rewritten in terms of the fluctuating modes p', u', and T_o' as

$$\frac{e'}{E_b} = S_p \frac{p'}{P} + S_u \frac{u'}{U} - S_T \frac{T_o'}{T_o} \tag{35}$$

where the sensitivities are given by

$$S_p = \frac{1}{2} \frac{\partial(\ln Nu_o)}{\partial(\ln Re_\infty)} \tag{36}$$

$$S_u = \frac{1}{2}\left[\alpha_1 S_p - \frac{1}{\alpha_o \tau_{wr}} \frac{\partial(\ln \eta)}{\partial(\ln M)}\right] \tag{37}$$

$$S_T = \frac{1}{2}\left[\left(1 + \frac{m_o}{\alpha_o} - \frac{\alpha_1}{2}\right) S_p + S_u + \frac{1}{\tau_{wr}} + \frac{\partial(\ln Nu_o)}{\partial(\ln \theta)} - n_o\right] \tag{38}$$

As shown previously in figure 9, temperature recovery ratio is relatively independent of free-stream Reynolds number and is eliminated in the above sensitivity equations. Comparing probe sensitivity equations (19), (20), and (21) with equations (36), (37), and (38) indicates that the sensitivity to temperature increases to account for density fluctuations, while the sensitivity to velocity remains unchanged and the sensitivity to pressure is equivalent to that for density. Thus, based on prior observations with density, the pressure sensitivity can be assumed to be independent of temperature loading, and equation (35) after squaring and averaging can be written as

$$\frac{\overline{e_c'^2}}{E_b^2} = S_u^2 \frac{\overline{u'^2}}{U^2} - 2S_u S_T \frac{\overline{u'T_o'}}{UT_o} + S_T^2 \frac{\overline{T_o'^2}}{T_o^2} \tag{39}$$

where

$$\overline{e_c'^2} = \overline{\left(e' - e_p'\right)^2} \tag{40}$$

$$e_p' = E_b S_p \frac{p'}{P} \tag{41}$$

Equation (39) can be solved as before by using equation (26) or by the graphical modal analysis method of Kovásznzy (1953). In either case, the fluctuating voltage contribution due to pressure e'_p must be estimated from fluctuating static pressure measurements or assumed to be negligible. If estimated, the associated pressure measurements must be accomplished in real time to preserve the required phase information between e' and e'_p.

The right-hand side of equation (39) can be put into a more convenient form as previously shown by Kovásznzy (1953). With the following definitions,

$$\langle e_c \rangle = \sqrt{\overline{e'^2_c}}\Big/E_b \qquad \langle u \rangle = \sqrt{\overline{u'^2}}\Big/U$$

$$\theta^{*2}_c = \langle e_c \rangle^2 / S_T^2 \qquad \langle T_o \rangle = \sqrt{\overline{T'^2_o}}\Big/T_o \tag{42}$$

$$r = S_u/S_T \qquad R_{uT_o} = \overline{u'T'_o}\Big/\sqrt{\overline{u'^2}}\sqrt{\overline{T'^2_o}}$$

equation (39) can be given as

$$\theta^{*2}_c = \langle u \rangle^2 r^2 - 2R_{uT_o}\langle u \rangle \langle T_o \rangle r + \langle T_o \rangle^2 \tag{43}$$

Equation (43) has the same functional form as that for the cylindrical sensor. Either Kovásznzy's graphical modal analysis method or equation (26) can be used to solve equation (43). At least three temperature overheats are required to solve for the coefficients $\langle u \rangle$, $\langle T_o \rangle$, and R_{uT_o} appearing in equation (43). A typical example of application of equation (43) can be found in Seiner and Yu (1981), who studied the turbulence properties of an unheated shock-containing supersonic jet plume. In their work, however, they assumed that $e'_p \approx 0$.

ASSOCIATED PROPERTIES OF HOT-FILM PROBES

Directional Response of Probe

A quantity of great interest to theoreticians and experimentalists alike is the variation of the turbulent Reynolds stress tensor (i.e., $\overline{u'_i u'_j}$) in supersonic free jet and boundary layer flows. In certain fluid dynamic problems, this stress tensor may be obtained from a predetermined sampling method to obtain, for example, coherent structure within the flow. Probes designed for Reynolds stress measurements have two sensors angled to the probe axis. Thus, the directional response of the wedge probe was examined.

Only partial results have been obtained for the wedge probe; however some interesting similarities exist between its directional response and that of the cylindrical hot-film probe. Figures 22 and 23 respectively show the yaw directional response for the cylindrical and wedge probes. In both cases, the data are normalized by data at the normal flow angle of $\phi = 0°$. On the basis of the dimensions given in figure 2, the cylindrical probe has an aspect ratio (L/D) of only 43. According to the experimental results of Champagne, Sleicher, and Wehrmann, (1967), heat conduction losses are of greater significance with small aspect ratio probes, since the convective heat transfer is reduced by the factor ($\cos \phi$). For very high aspect ratio probes where $L/D > 600$, they found that the cosine law is adequate to describe the directional response of a hot wire. With small aspect ratios, their data empirically correlated according to

$$Nu_o(\phi) = Nu_o(\cos^2\phi + k^2 \sin^2\phi) \tag{44}$$

Their data were obtained at a low subsonic speed of 35 m/sec, and for probes with L/D = 200 to 600, the parameter k respectively varied nonlinearly from 24 to 0. The cylindrical hot-film data in figure 22 are compared with those given by equation (44), the solid line representing $k = 0$ and the dashed line representing $k = 0.95$. The data at supersonic speeds closely follow the cosine law behavior (i.e., $k = 0$), but the data at subsonic and sonic speeds show poor directional response. This can be attributed perhaps to conduction losses, as suggested by equation (44), or to peculiar transonic effects.

The wedge probe data of figure 23 also show poor directional behavior when compared with the cosine law at subsonic and sonic speeds. While one might expect the wedge probe to have improved directional behavior at supersonic speeds, as does the cylindrical probe, further investigation is required before use of dual sensor wedge probes for Reynolds stress measurements.

Probe Frequency Response and Durability

The frequency response of the wedge probe was examined by performing the standard square wave insertion test while the probe was operated in a supersonic stream under balanced conditions. With a 1-to-1 bridge ratio, this test indicated that the frequency response was near 130 kHz for probe Z. In addition to this test, the recent results of Seiner, McLaughlin, and Liu (1982) show that the response is at least 40 kHz since these measurements demonstrate the existence of a universal mixing layer spectrum for the initial mixing layer associated with the flow from the Mach 2 nozzle. The durability of the probe is remarkable compared with cylindrical sensors from the standpoint that none of the electrical parameters of wedge probes degrade with long-term use. Also wedge probes survive in severe flow environments, whereas cylindrical probes are subject to failure in the turbulent shear zones of supersonic flow.

Probe Limitations and Associated Difficulties

The method adopted for analysis of the wedge hot-film probe follows the local linearization method introduced by Kovásznay (1950 and 1953) and Morkovin (1956) for hot-wire probes. As such, the method is limited to turbulence measurements where the

local turbulence intensity is a small percentage of the mean flow. Thus significant errors can occur when the local turbulence intensity level exceeds 20 percent.

The major disadvantage of operating the wedge hot-film probe is that auxiliary measurements are required to determine the local free-stream Mach number if not known a priori. In addition, when pressure or density fluctuations cannot be assumed negligible, then the fluctuating static pressure must also be obtained concomitantly with wedge hot-film measurements. Cylindrical hot-wire or hot-film probes have a similar problem in the transonic flow range, but for supersonic free-stream Mach numbers exceeding 1.3, these problems are avoided because the cylindrical probe has the same sensitivity to density as to velocity and these sensitivities are independent of the free-stream Mach number. Unfortunately, the cylindrical probe cannot withstand high Reynolds number supersonic flows, like the ones Seiner and Yu (1981) and Seiner, McLaughlin, and Liu (1982) considered.

CONCLUSIONS

This report has examined the response obtained with a wedge hot-film probe in transonic and low supersonic flow with high unit Reynolds numbers of 20×10^6 to 280×10^6 per meter. The results of this study showed that the wedge probe response depends on Mach number through the entire flow range when correlated with a Reynolds number based on stagnation temperature conditions. When correlated with a Reynolds number based on the free-stream static temperature conditions, the dependence of the probe response on Mach number is appropriately absorbed.

Based on this result, appropriate sensitivities to density, velocity, and temperature fluctuations were derived for the wedge probe according to local linearization method of Kovásznay and Morkovin. Examination of the variation of these sensitivity coefficients with the flow parameters showed that it is possible to neglect the dependence of the temperature recovery ratio on free-stream Reynolds number and that unlike the cylindrical probe response above Mach 1.3, the wedge probe sensitivity to velocity is generally always larger than its sensitivity to density. This result has a far-reaching effect on methods used to interpret the wedge probe voltage response, since one is forced to solve for all three modal fluctuations.

Examination of the variation of the wedge probe modal sensitivities with temperature loading showed that the density sensitivity was virtually independent of temperature loading. Inclusion of the density sensitivity in the probe transformation matrix produced irregular results that were directly attributed to the weak dependence of the density sensitivity on temperature loading. On the basis of this finding, it was concluded that until more accurate anemometry instrumentation becomes available, the fluctuating flow variables can only be determined to within an arbitrary factor. The paper shows, however, that with a concomitant measure of the fluctuating static pressure, both the fluctuating velocity and temperature modes can be determined from the wedge hot-film voltage fluctuations. This represents the recommended procedure to be used for analyzing the wedge hot-film response.

Heat conduction losses for the wedge hot-film probe were not explicitly treated in this paper. However, a one-dimensional estimate for heat conduction losses along with an empirical heat transfer law for hot wires with end conduction loss correction indicated that the hot-film cylindrical sensor has small end conduction losses at high Reynolds numbers. Extension of this estimate to the wedge probe geometry repre-

sents an important area for further research, since even small conduction end loss corrections can strongly influence the behavior of the wedge probe transformation matrix.

The directional responses for both cylindrical and wedge hot-film probes indicate that near sonic conditions, neither probe type produced adequate response for Reynolds stress measurements. With supersonic free-stream Mach numbers and low turbulence levels, the cylindrical hot-film probe exhibited good directional response. Additional research is required to define the directional response of the wedge probe beyond the sonic condition.

Even though the wedge probe requires auxiliary measurements to determine either fluctuating static pressure or fluctuating density and to determine local free-stream Mach number, it offers a means whereby the fluctuating velocity, temperature, and their mutual correlation can be obtained with good frequency response ($\approx$130 kHz). This represents an attractive feature, for these multiple modes have thus far been modeled in high Reynolds number supersonic flows by empirical methods in the absence of any confirming experimental data. The wedge hot-film probe represents a complementary system to the laser velocimeter for supersonic flow measurements.

As a final note, the response of the wedge hot-film probe in transonic to low supersonic flows should not be extrapolated to other wedge geometries and flow regimes without careful investigation. In this paper, a 40° semivertex wedge angle was studied, and the results indicated that its heat transfer properties depended on Mach number even though the bow shock is detached throughout the supersonic flow range investigated. Certainly one would expect that with increasing bow shock angles, the wedge probe would begin to behave like the cylindrical probe whose bow shock is always detached. It would be of substantial importance to examine a wedge probe with a larger semivertex angle or one fitted with a rounded nose.

Langley Research Center
National Aeronautics and Space Administration
Hampton, VA 23665
March 2, 1983

APPENDIX

CONDUCTION END LOSS ESTIMATE FOR THE CYLINDRICAL HOT-FILM PROBE

Figure 2 illustrates the cross section of cylindrical hot-film probe. The complex geometry associated with the various material layers clearly suggests the use of a numerical approach to solve for heat transferred by conduction. However, as is shown below using a one-dimensional approximation, the numerical approach is not necessary because the heat transferred by conduction represents a small fraction of the total heat transferred for probes operating at high Reynolds numbers. The one-dimensional estimate assumes that the primary mode of heat transfer by conduction is through the thin nickel film. This assumption is justified on the basis that the thermal conductivity of nickel is approximately 100 times that of the quartz fiber. The energy equation for this problem is given by

$$\frac{I^2 R_a}{2L}[1 + \alpha(T - T_a)] = \pi D h_c (T - T_r) - \left(\frac{\pi D^2 k_o}{4}\right)\frac{d^2 T}{dx^2} \tag{A1}$$

where R_a is the probe resistance at ambient temperature T_a and the value selected for D is the diameter representing an equivalent cross-sectional area for the nickel film. In equation (A1), I represents the electrical current flowing through the film, and T represents the temperature of the nickel along the cylinder axis x. For the probe illustrated in figure 2, the equivalent probe diameter is $D = 11.5$ μm. Solution of the above equation, subject to $T = T_r$ at $x = L$ and $dT/dx = 0$ at $x = 0$, provides the following estimate for heat transferred by convection Q_c and conduction Q_k:

$$Q_c = 2\pi D L h_c b_2 \left\{1 - \left[\frac{\tanh\left(\sqrt{b_1} L\right)}{\sqrt{b_1} L}\right]\right\} \tag{A2}$$

$$Q_k = \frac{\pi}{2} D^2 k_o b_2 \sqrt{b_1} \tanh\left(\sqrt{b_1} L\right) \tag{A3}$$

where

$$b_1 = \frac{4\pi L D h_c - 2\alpha I_p^2 R_a}{\pi L D^2 k_o} \tag{A4}$$

$$b_2 = \frac{I_p^2 R_a [1 + \alpha(T - T_a)]}{2\pi L D h_c - \alpha I_p^2 R_a} \tag{A5}$$

Both Q_c and Q_k can be solved for numerically by determining the convective heat transfer coefficient h_c from the probe calibration data. These results are shown in figure 24. The results in this figure show that in terms of the parameter $\varepsilon = Q_k/(Q_c + Q_k)$, the heat transferred by conduction is of less significance with increasing probe Reynolds number and temperature overheat. The Reynolds number is based on the actual 70-μm diameter of the hot-film probe. The one-dimensional model estimate in figure 24 illustrates that heat conduction is relatively small in the high probe Reynolds number range of this study. The lower set of data in figure 24(c) is for the highest Mach number (i.e., $M = 2.0$).

REFERENCES

Behrens, Wilhelm 1971: Total Temperature Thermocouple Probe Based on Recovery Temperature of Circular Cylinder. Int. J. Heat & Mass Transfer, vol. 14, no. 10, pp. 1621-1630.

Champagne, F. H.; Sleicher, C. A.; and Wehrmann, O. H. 1967: Turbulence Measurements With Inclined Hot-Wires. Pt. 1. Heat Transfer Experiments With Inclined Hot-Wire. J. Fluid Mech., vol. 28, pt. 1, pp. 153-175.

Glaznev, V. M. 1973: Some Features of the Propagation of a Discrete Tone Perturbation in a Free Supersonic Jet. Fluid Mech. - Soviet Res., vol. 2, no. 3, pp. 76-79.

Ho, C. L.; McLaughlin, D. K.; and Troutt, T. R. 1978: Supersonic Hot-Wire Fluctuation Data Analysis With a Conduction End-Loss Correction. J. Phys. E.: Sci. Instr., vol. 11, no. 5, pp. 488-494.

Horstman, C. C.; and Rose, W. C. 1977: Hot-Wire Anemometry in Transonic Flow. AIAA J., vol. 15, no. 3, pp. 395-401.

Kovásznzy, Leslie S. G. 1950: The Hot-Wire Anemometer in Supersonic Flow. J. Aeronaut. Sci., vol. 17, no. 9, pp. 565-572, 584.

Kovásznay, Leslie S. G. 1953: Turbulence in Supersonic Flow. J. Aeronaut. Sci., vol. 20, no. 10, pp. 657-674, 682.

Laufer, John; and McClellan, Robert 1956: Measurements of Heat Transfer From Fine Wires in Supersonic Flows. J. Fluid Mech., vol. 1, pt. 3, pp. 276-289.

Ling, S. C.; and Hubbard, P. G. 1956: The Hot-Film Anemometer: A New Device for Fluid Mechanics Research. J. Aeronaut. Sci., vol. 23, no. 9, pp. 890-891.

Lord, R. G. 1974: Hot-Wire Probe End-Loss Corrections in Low Density Flows. J. Phys. E.: Sci. Instr., vol. 7, no. 1, pp. 56-60.

Morkovin, Mark V. 1956: Fluctuations and Hot-Wire Anemometry in Compressible Flows. AGARDograph 24.

Seiner, J. M.; and Yu, J. C. 1981: Acoustic Near Field and Local Flow Properties Associated With Broad-band Shock Noise. AIAA-81-1975.

Seiner, John M.; McLaughlin, Dennis K.; and Liu, C. H. 1982: Supersonic Jet Noise Generated by Large-Scale Instabilities. NASA TP-2072.

TABLE I.- HOT-FILM PROBES

[R_L is 2.57 Ω for cylinder, 3.33 Ω for wedge; D is 70 μm for cylinder, 130 μm for wedge equivalent]

Probe type[a]	Designation	Description	α	R_a, Ω	L, mm
55R31	W	Wedge	0.0046	10.42	1.00
55R32	Y	Wedge	.0044	10.37	1.00
55R32	Z	Wedge	.0041	10.98	1.00
55R01	3	Cylinder	.0041	5.28	1.25

[a]Designation of DISA Electronics.

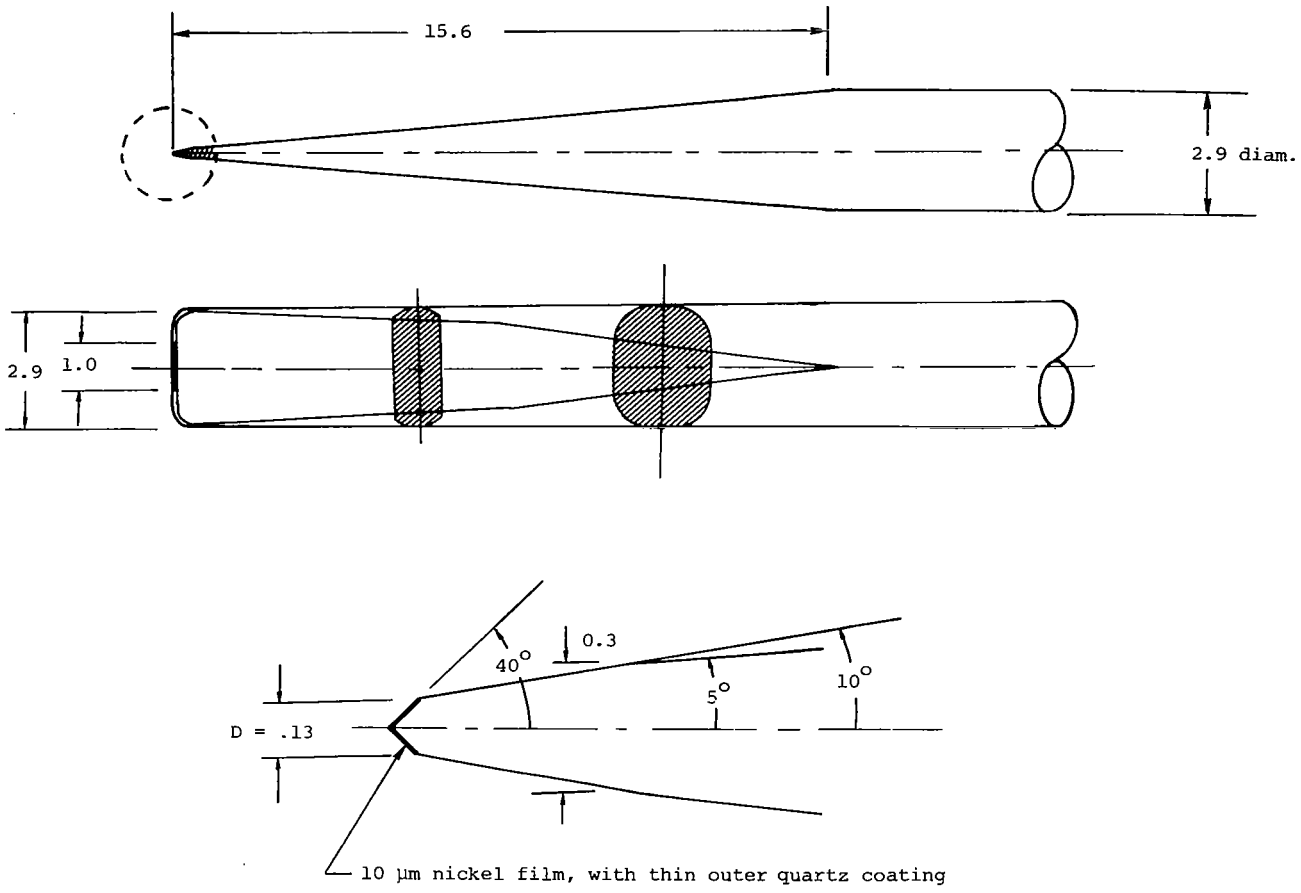

Figure 1.- Commercial hot-film wedge probe. Linear dimensions are in millimeters.

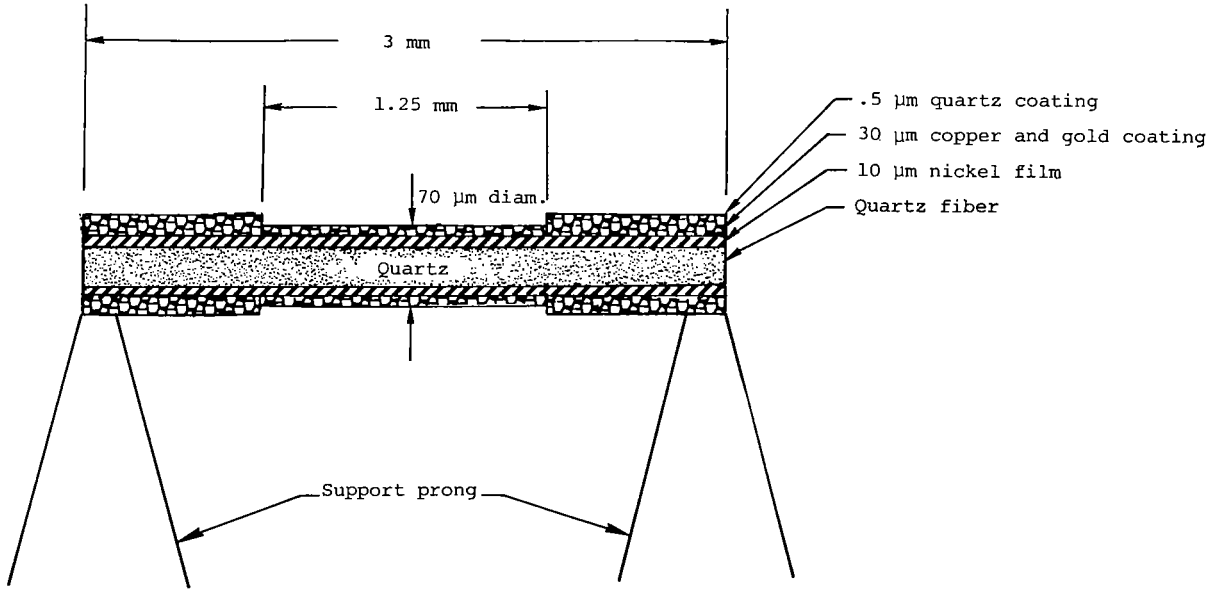

Figure 2.- Commercial hot-film cylindrical probe.

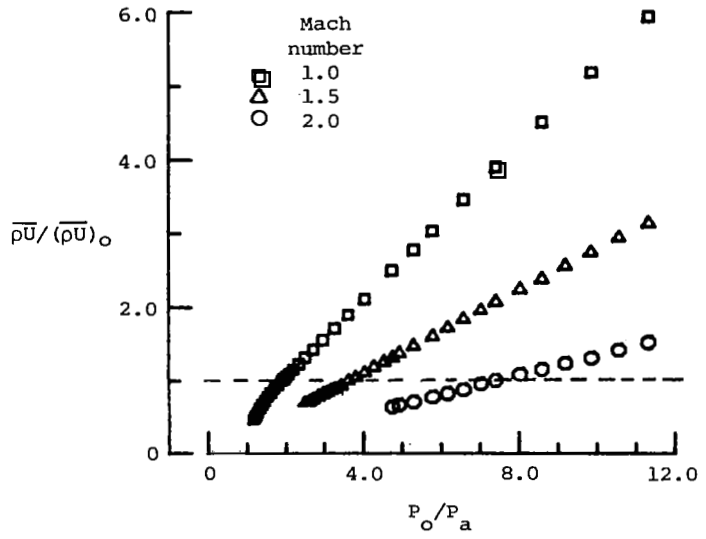

Figure 3.- Exit mean mass flux variation versus nozzle pressure ratio P_o/P_a for hot-film calibration.

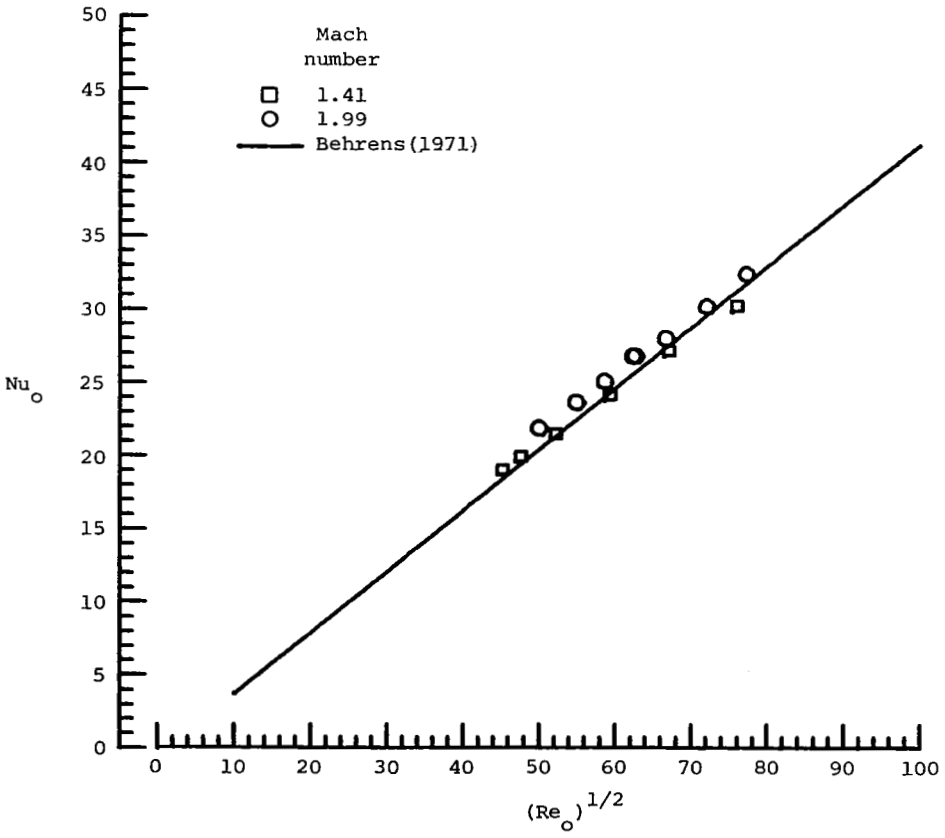

Figure 4.- Response of cylindrical hot-film probe 3 to Reynolds number. $\tau = 0.5$.

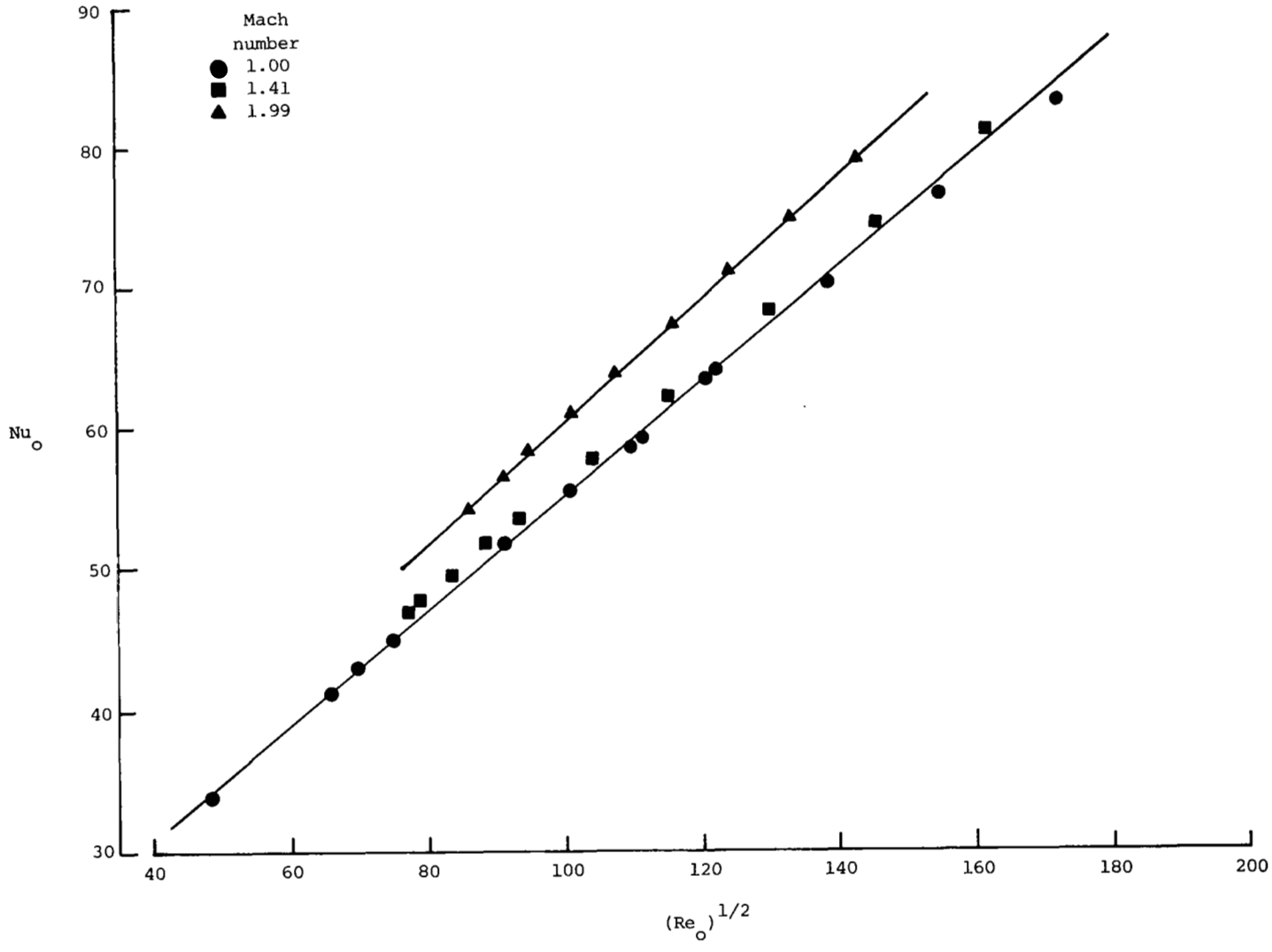

Figure 5.- Response of wedge hot-film probe Z to Reynolds number based on stagnation temperature. $\tau = 0.54$.

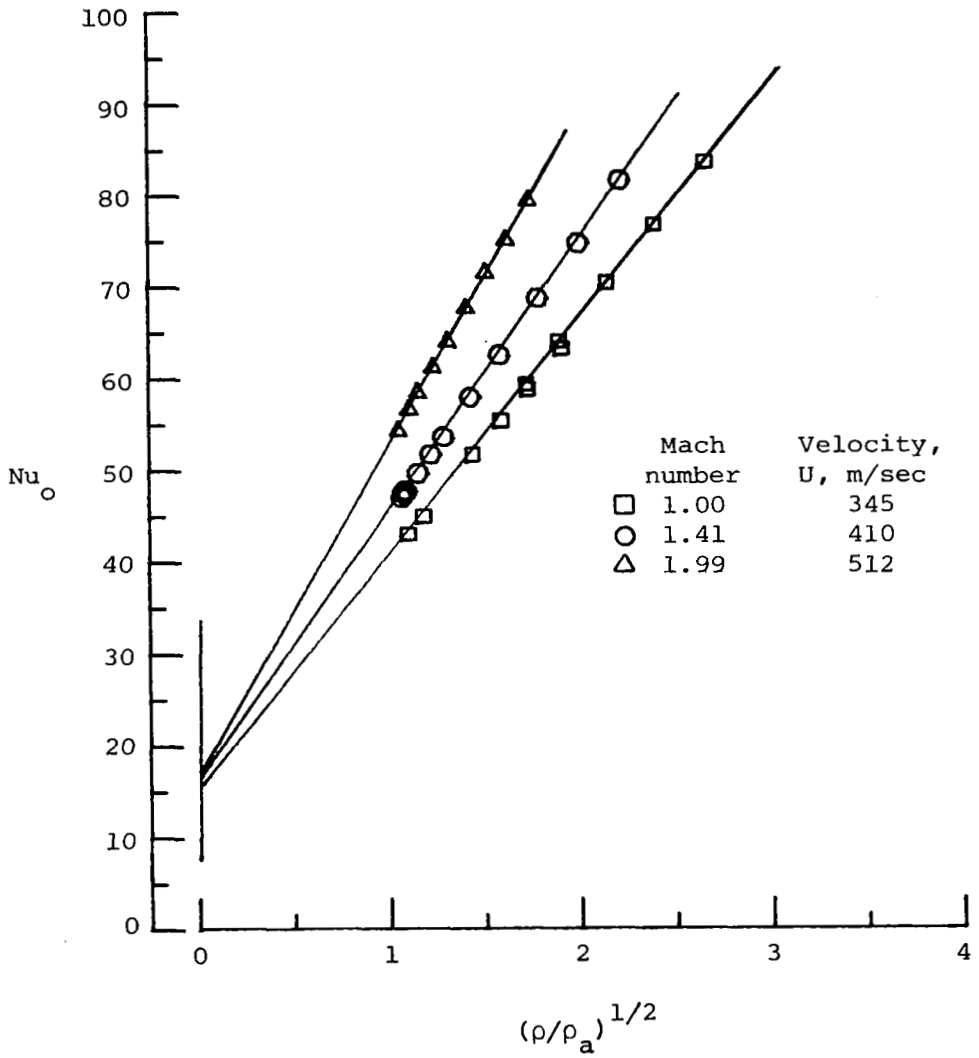

Figure 6.- Wedge hot-film probe response to density with velocity as a parameter. $\tau = 0.54$.

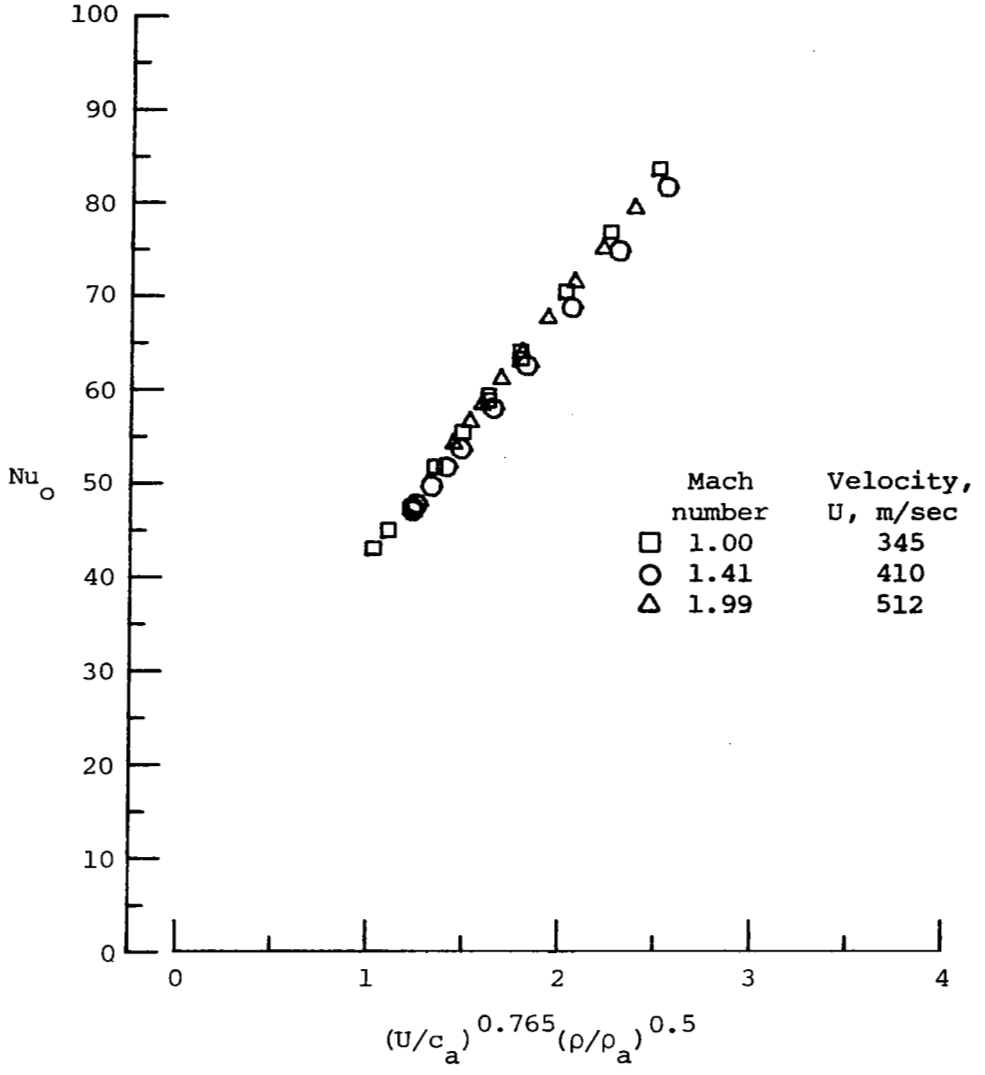

Figure 7.- Heat transfer correlation with velocity and density parameters. $\tau = 0.54$.

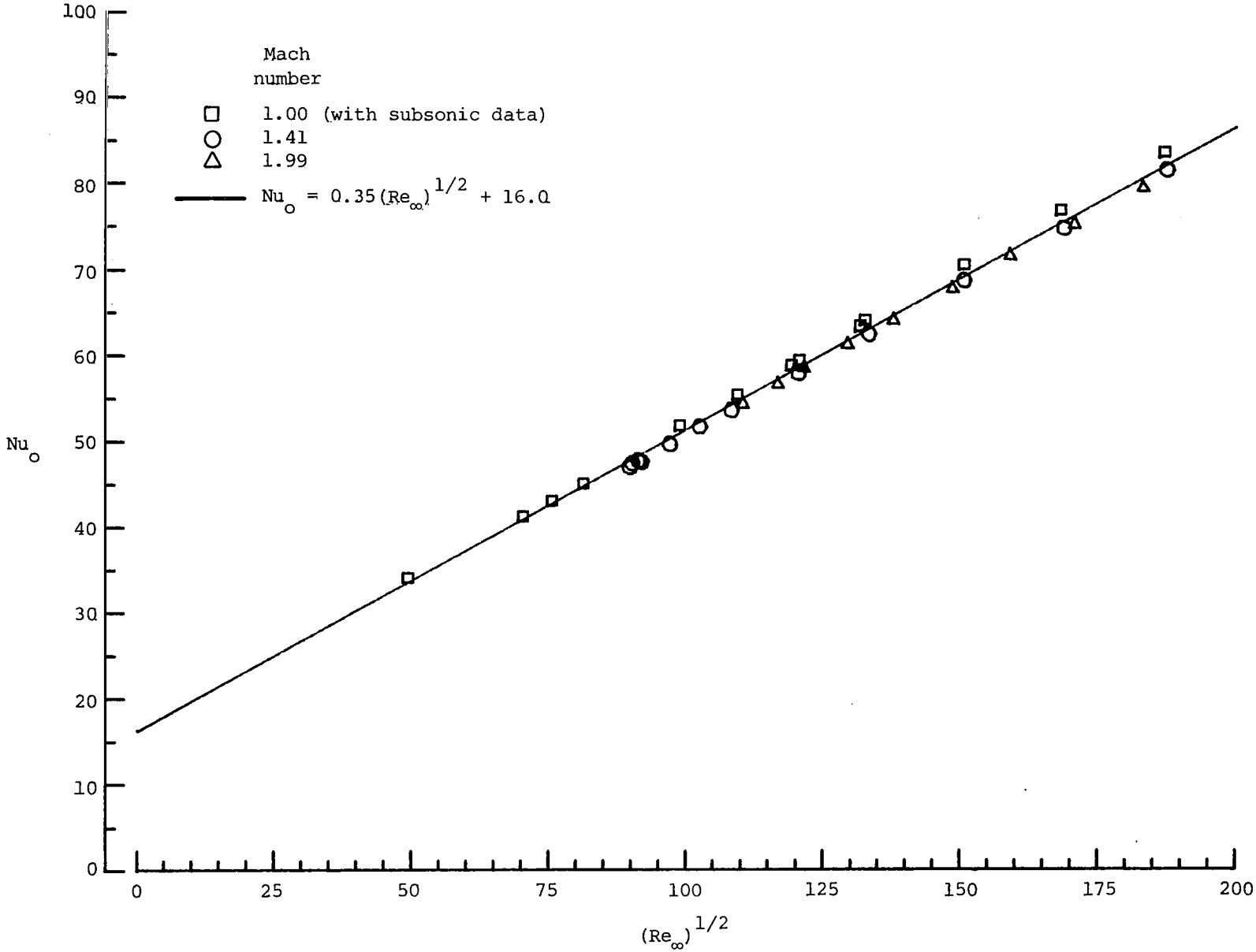

(a) Probe Z data; $\tau = 0.54$.

Figure 8.- Wedge hot-film probe response to Reynolds number based on free-stream temperature.

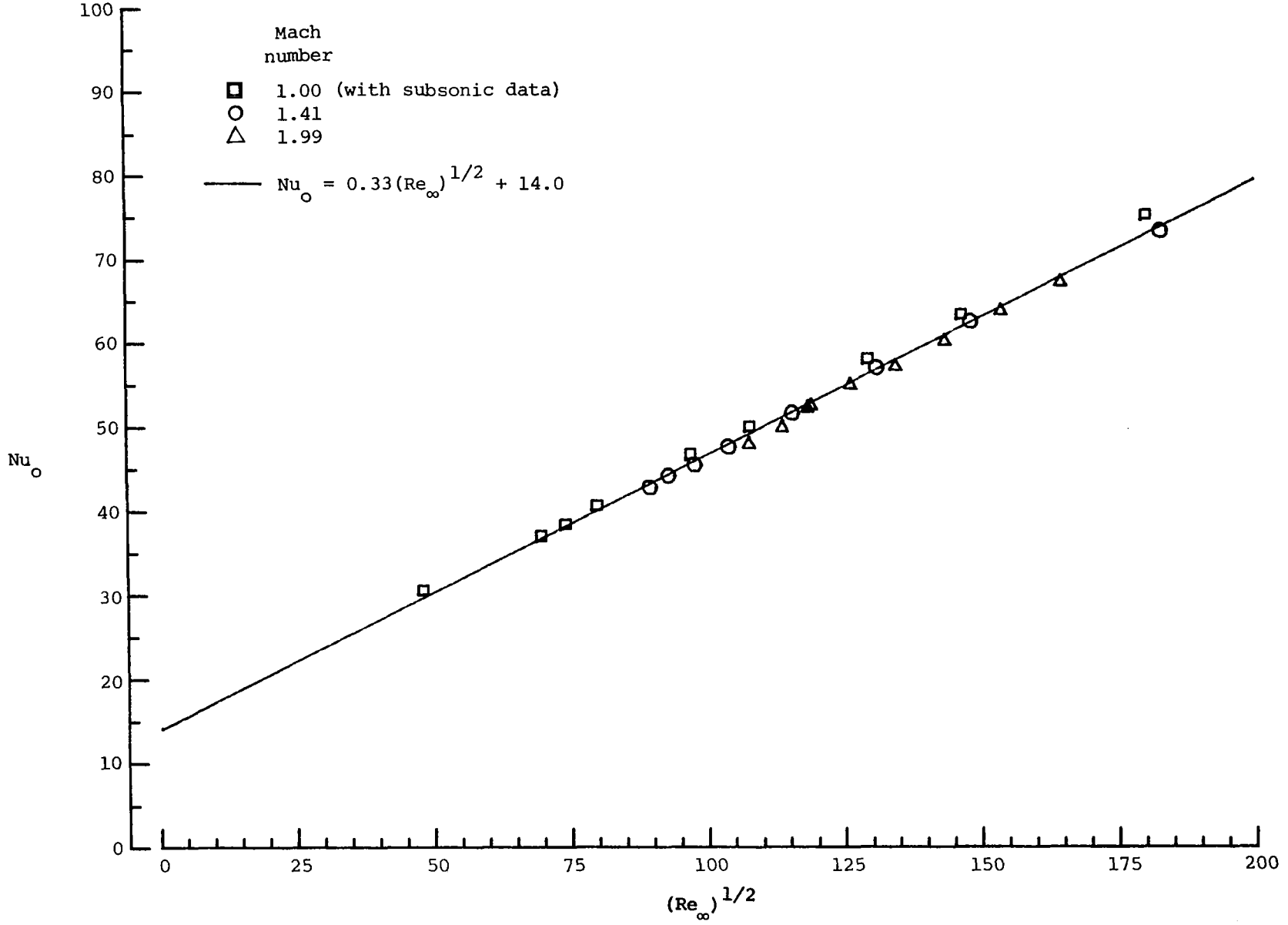

(b) Probe Y data; $\tau = 0.6$.

Figure 8.- Continued.

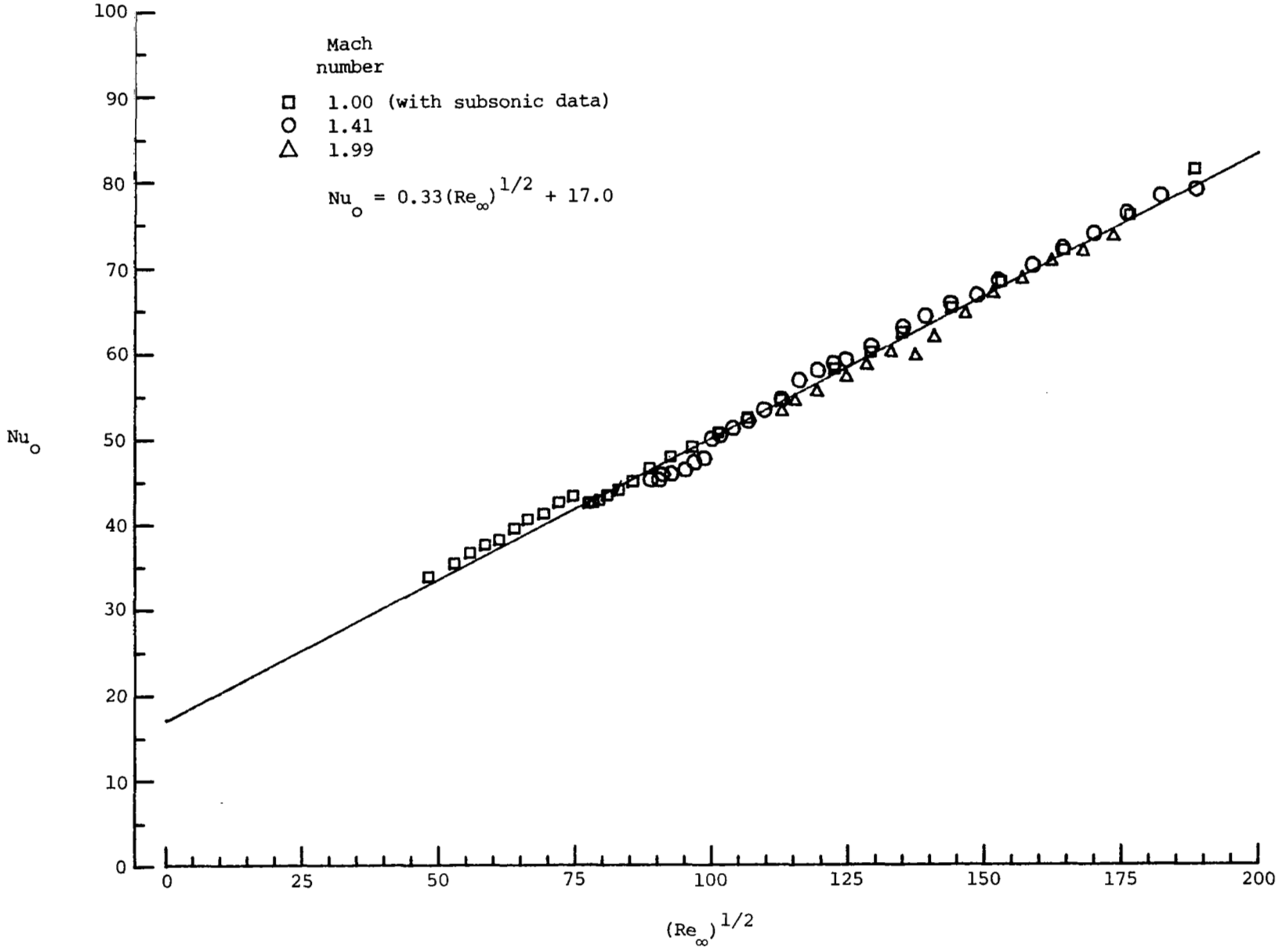

(c) Probe W data; $\tau = 0.99$.

Figure 8.- Concluded.

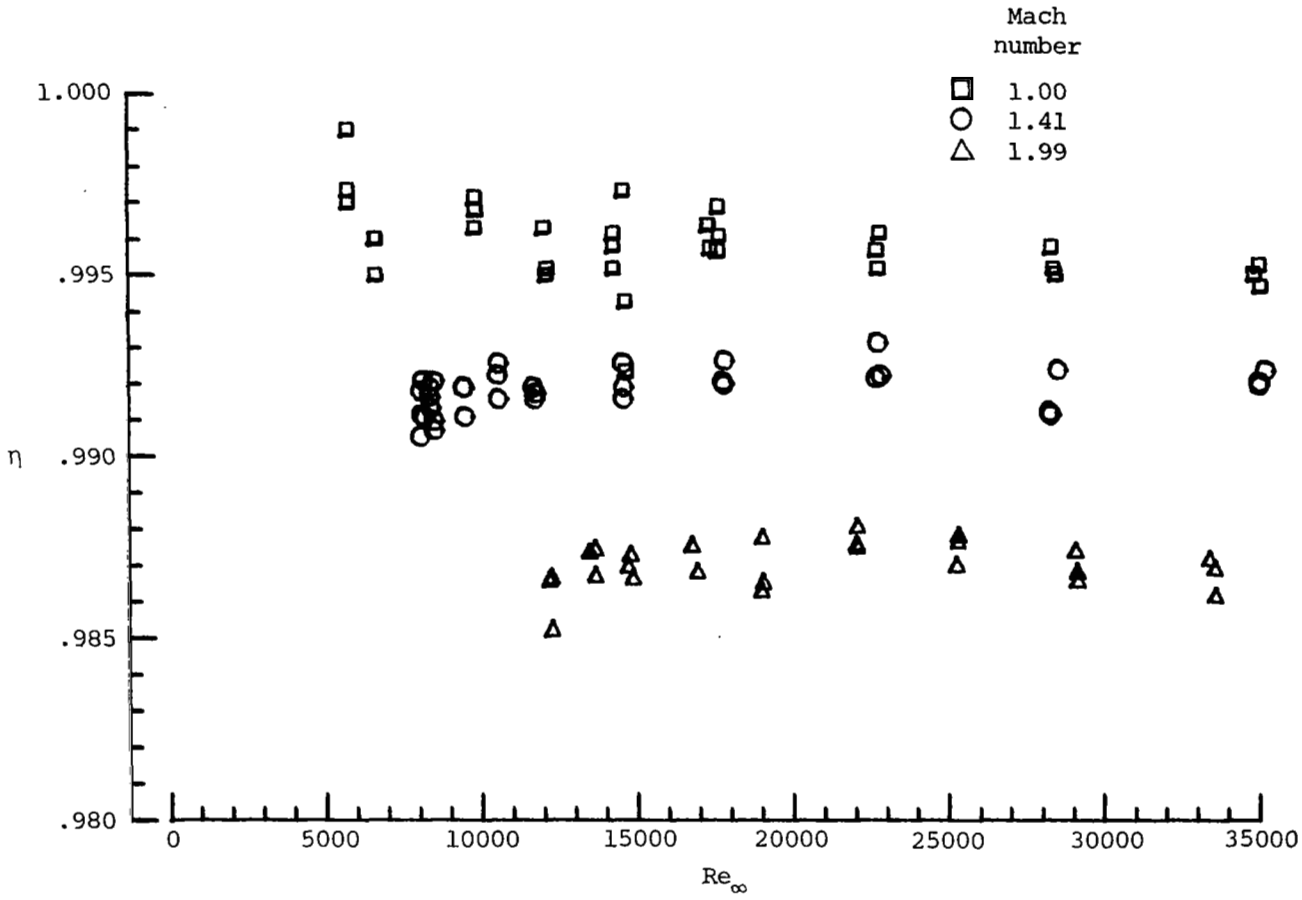

Figure 9.- Variation of temperature recovery ratio ($\eta = T_r/T_o$) with free-stream Reynolds number.

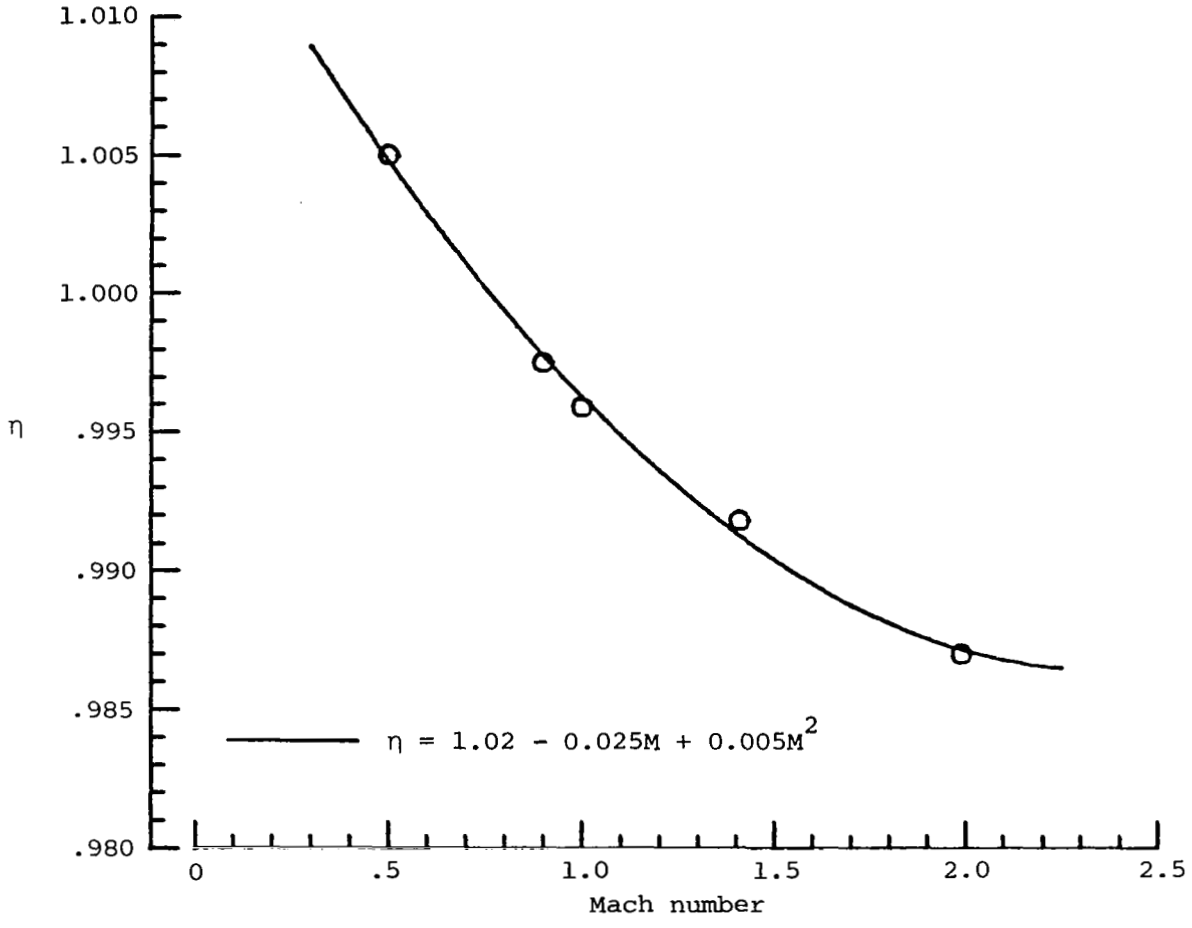

Figure 10.- Variation of temperature recovery ratio ($\eta = T_r/T_o$) with Mach number. Data points are averages over Reynolds number of η for each Mach number.

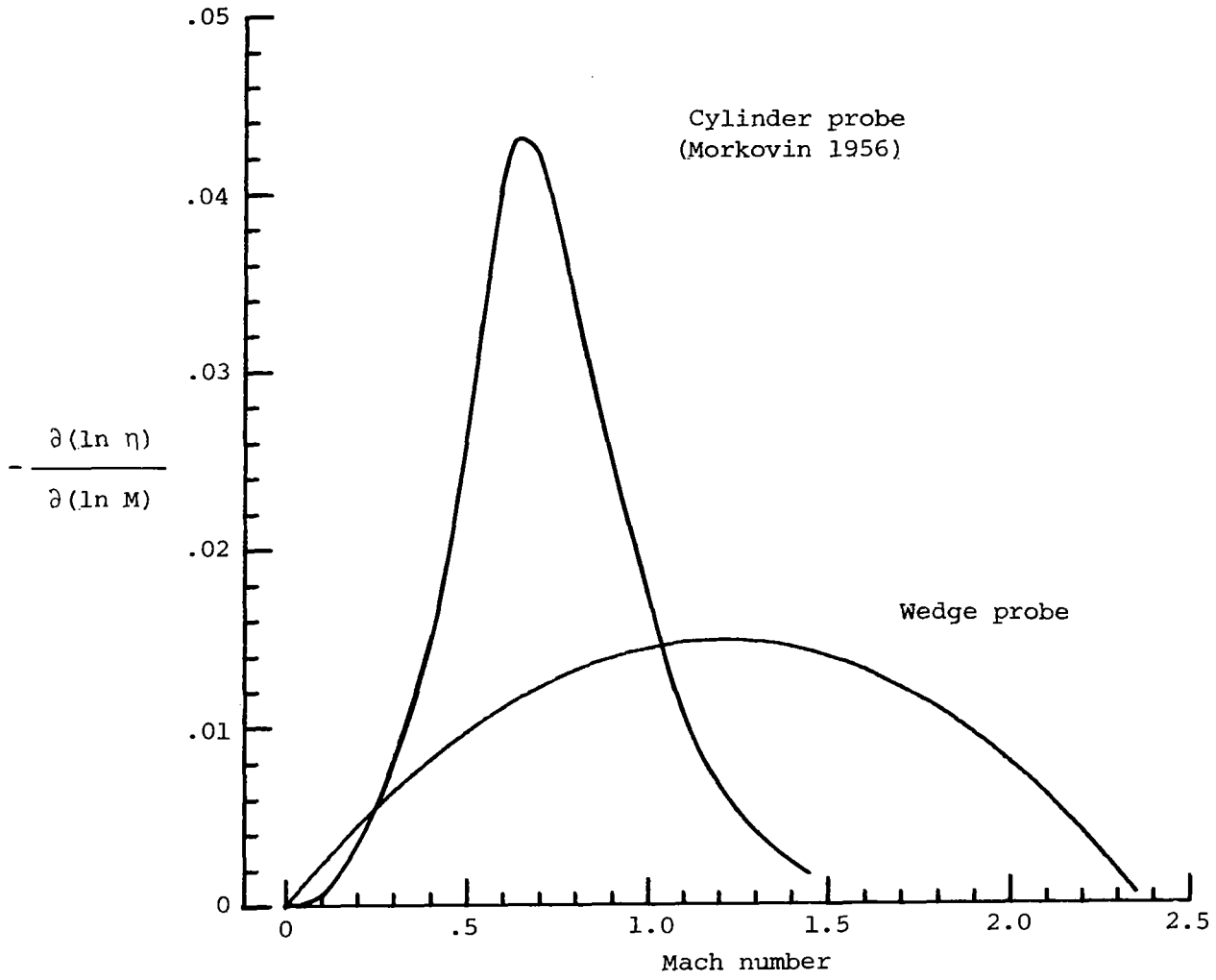

Figure 11.- Variation of logarithmic derivative of temperature recovery ratio with Mach number obtained from least squares representation in figure 10.

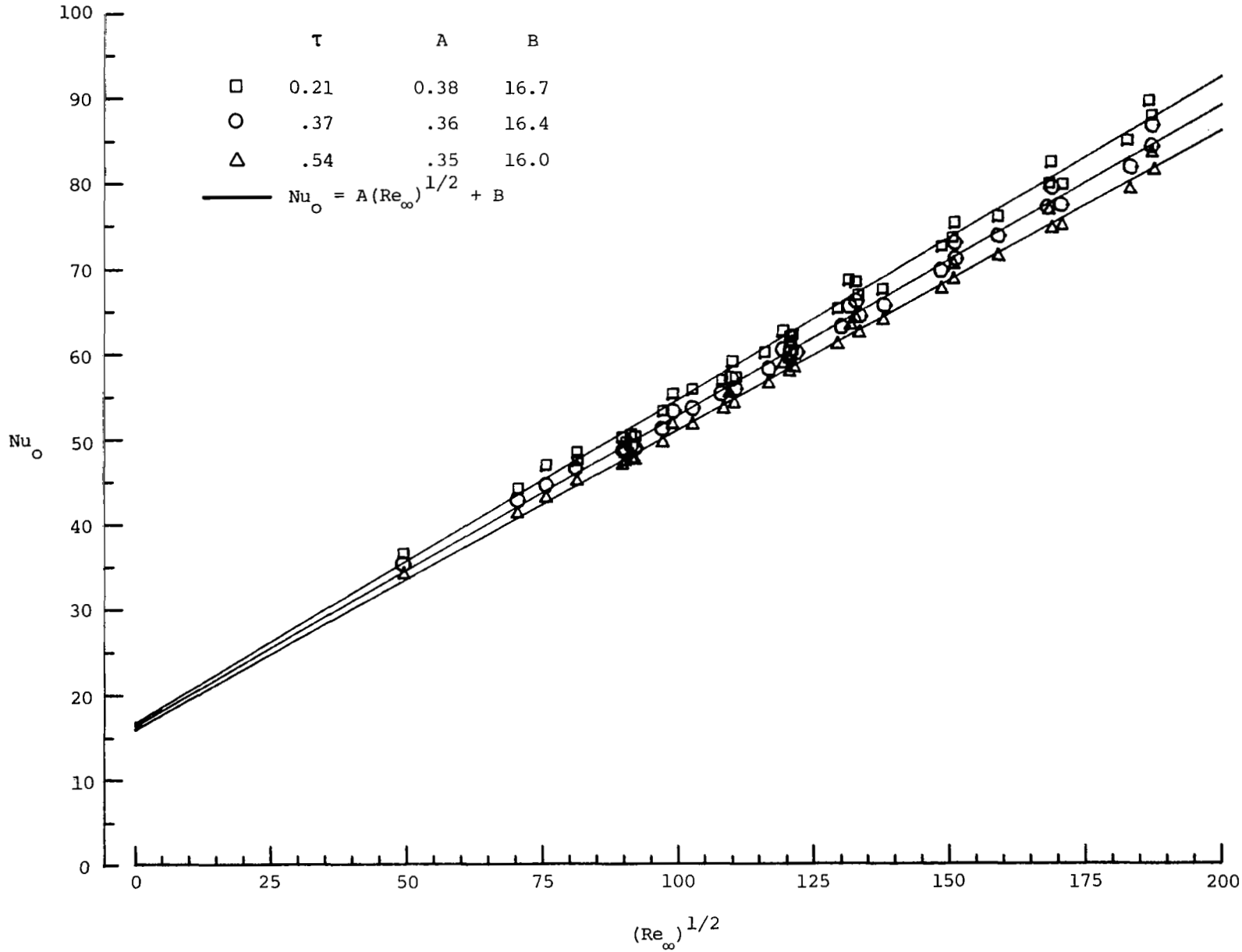

Figure 12.- Dependence of wedge hot-film probe response on temperature loading. Data for all Mach numbers included.

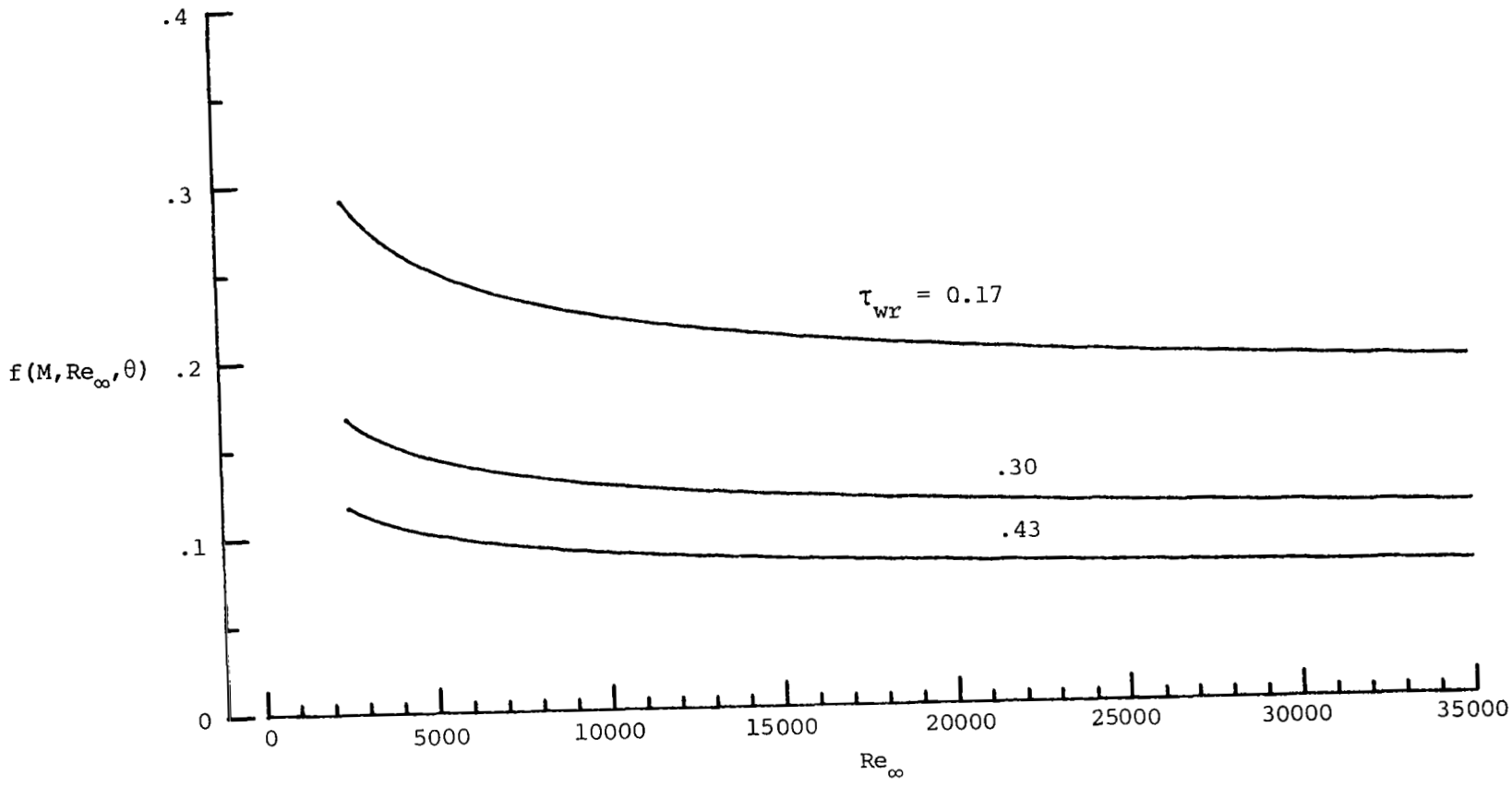

Figure 13.- Relative importance of the dependence of temperature recovery ratio on Mach number. M = 1.25.

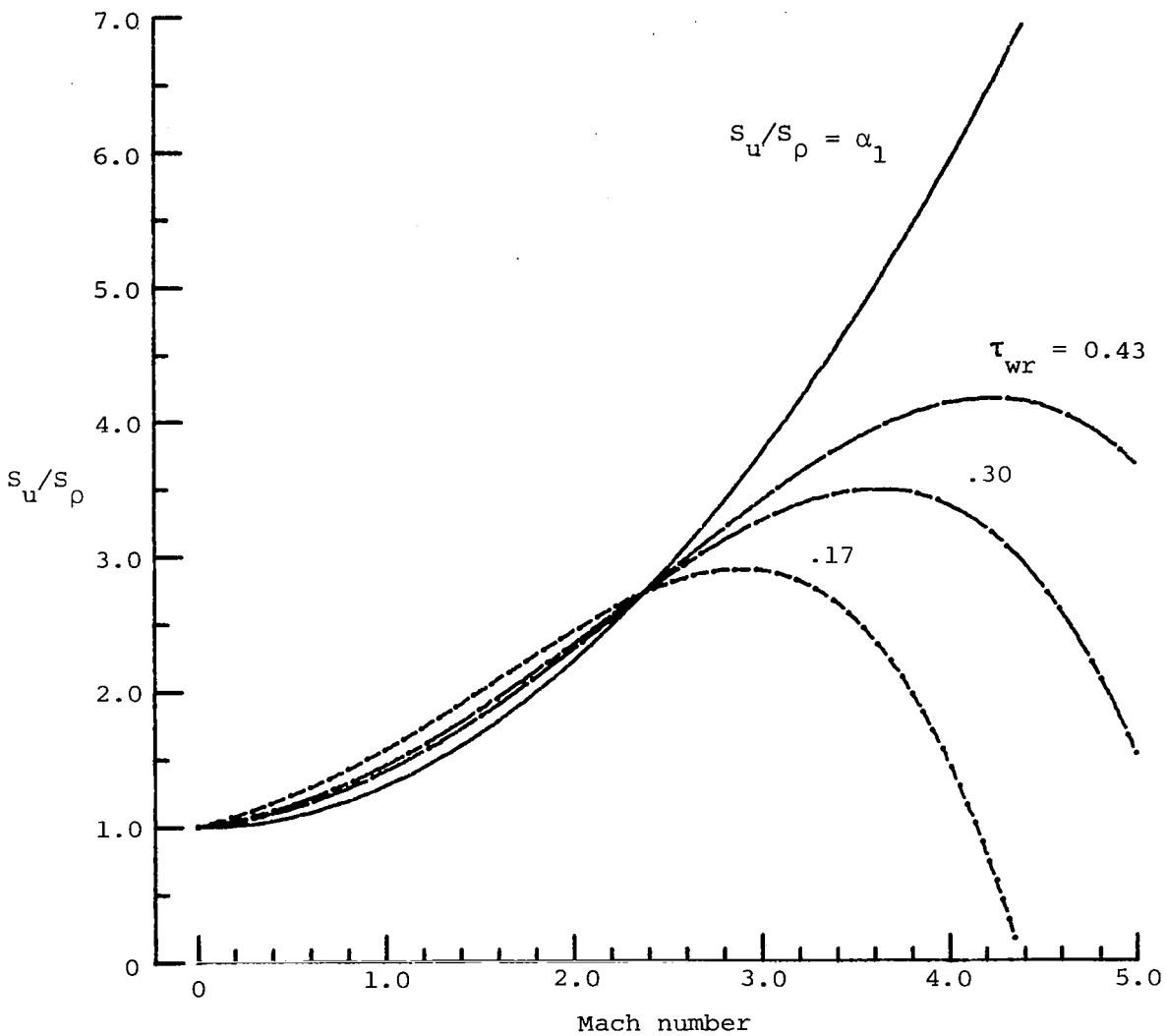

Figure 14.- Estimated variation of wedge probe velocity-to-density sensitivity ratio with Mach number for several temperature loadings. Re_∞ = 20000.

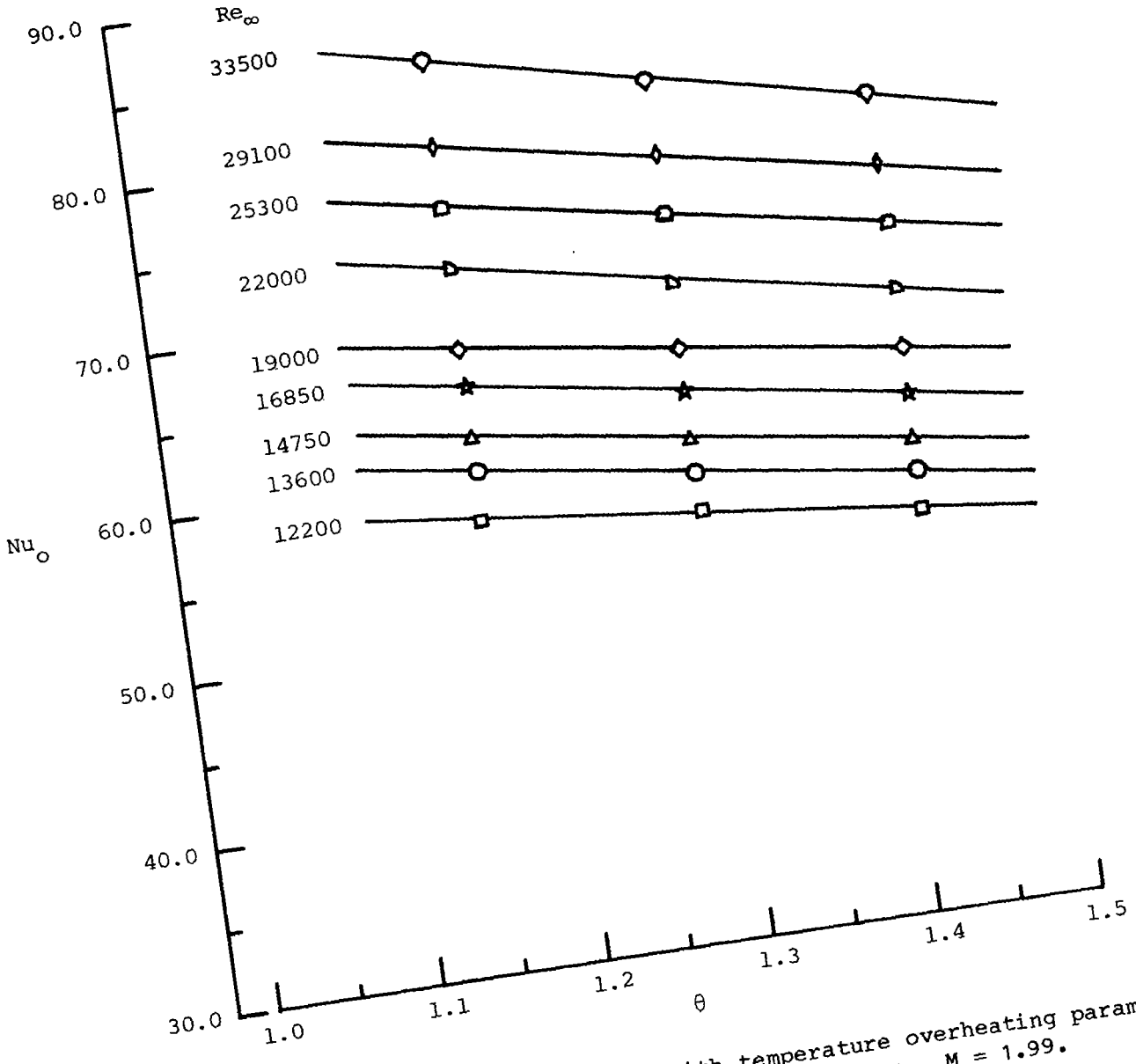

Figure 15.- Convective heat transfer behavior with temperature overheating parameter ($\theta = T_p/T_o$) for various free-stream Reynolds numbers. M = 1.99.

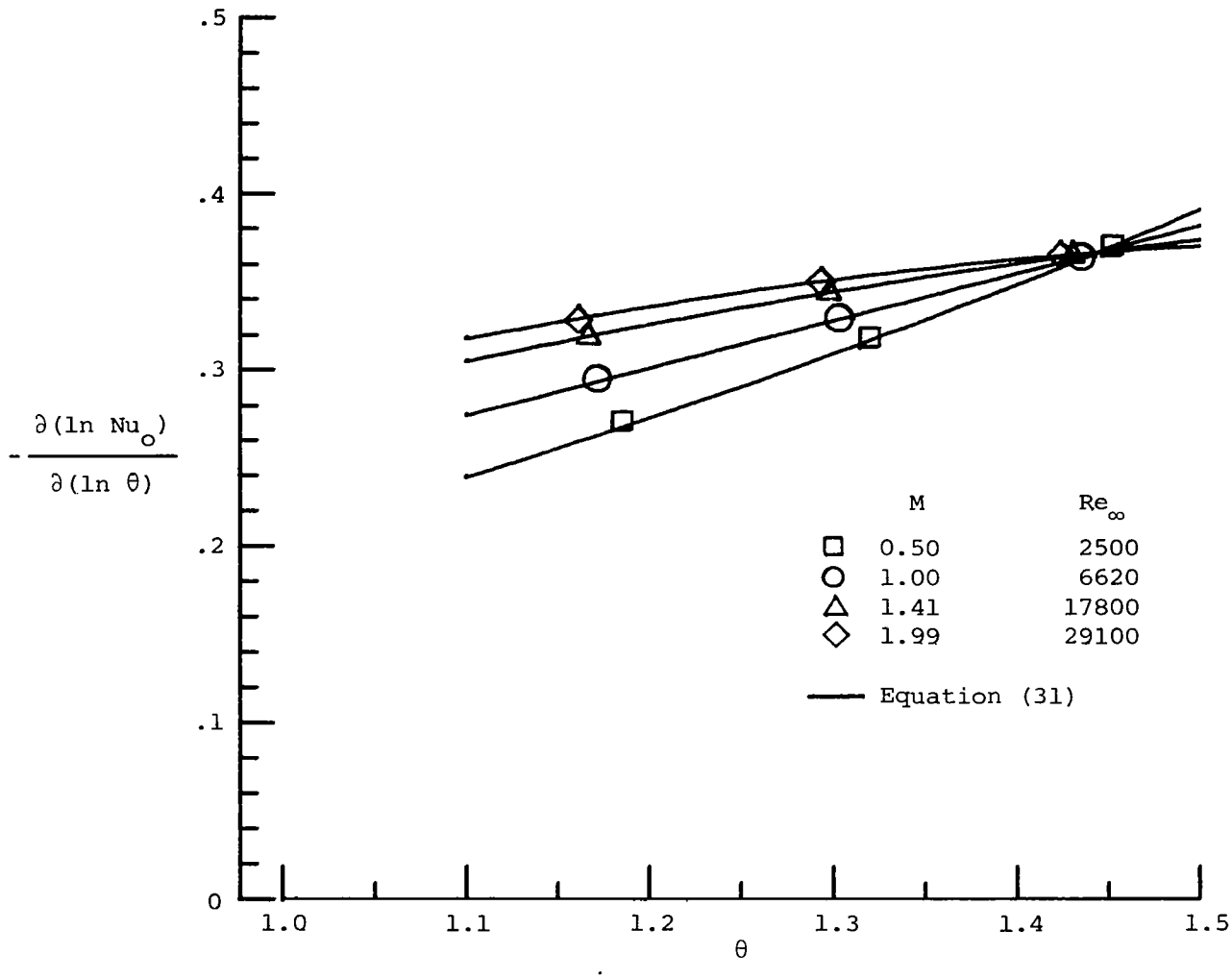

Figure 16.- Estimation of variation of logarithmic derivative of Nusselt modulus with temperature overheat.

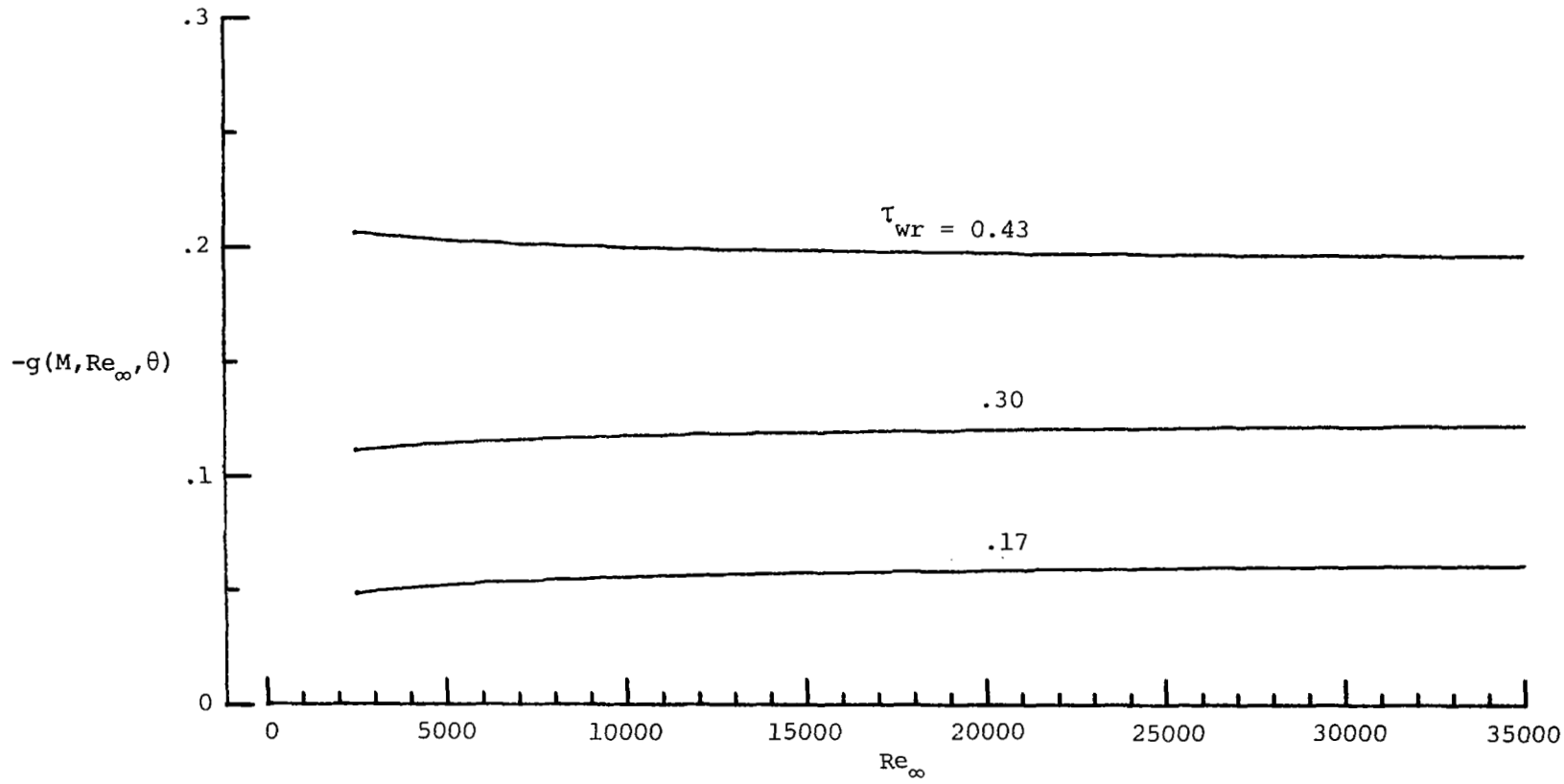

Figure 17.- Relative importance of dependence of logarithmic derivative of Nusselt modulus on temperature overheat. M = 1.25.

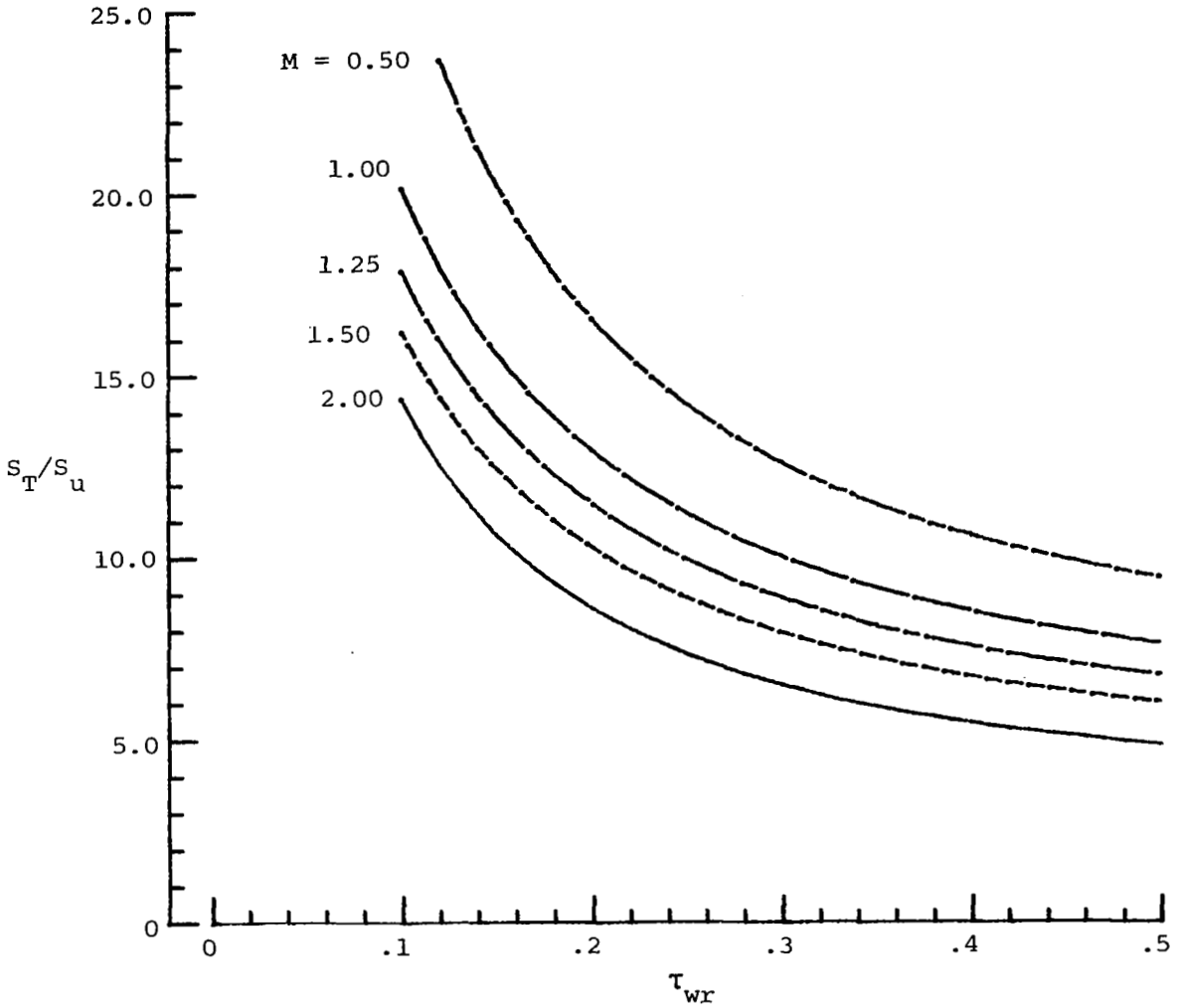

(a) $Re_\infty = 2500.$

Figure 18.- Estimated variation of temperature-to-velocity sensitivity ratio with temperature loading.

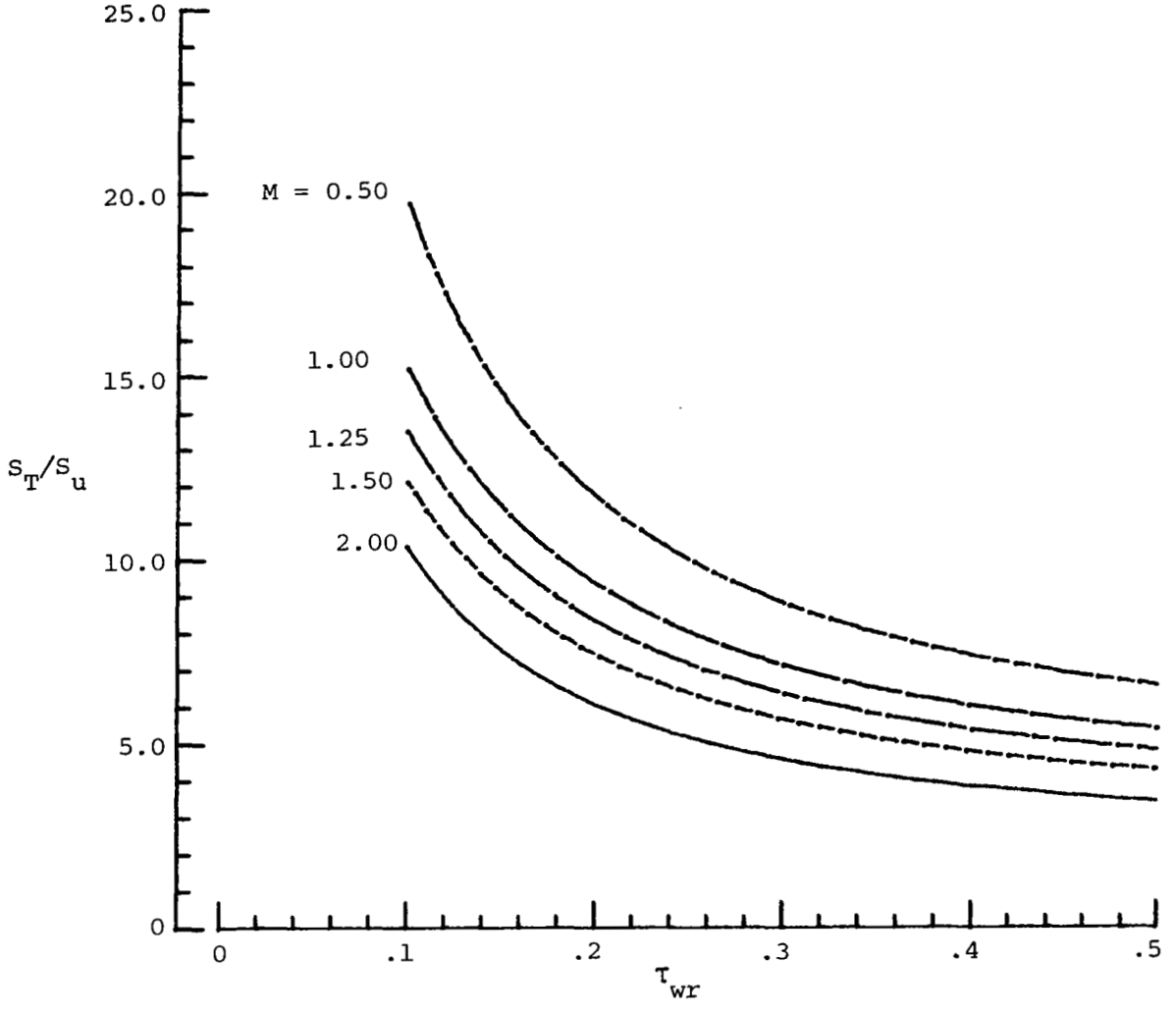

(b) $Re_\infty = 35000.$

Figure 18.- Concluded.

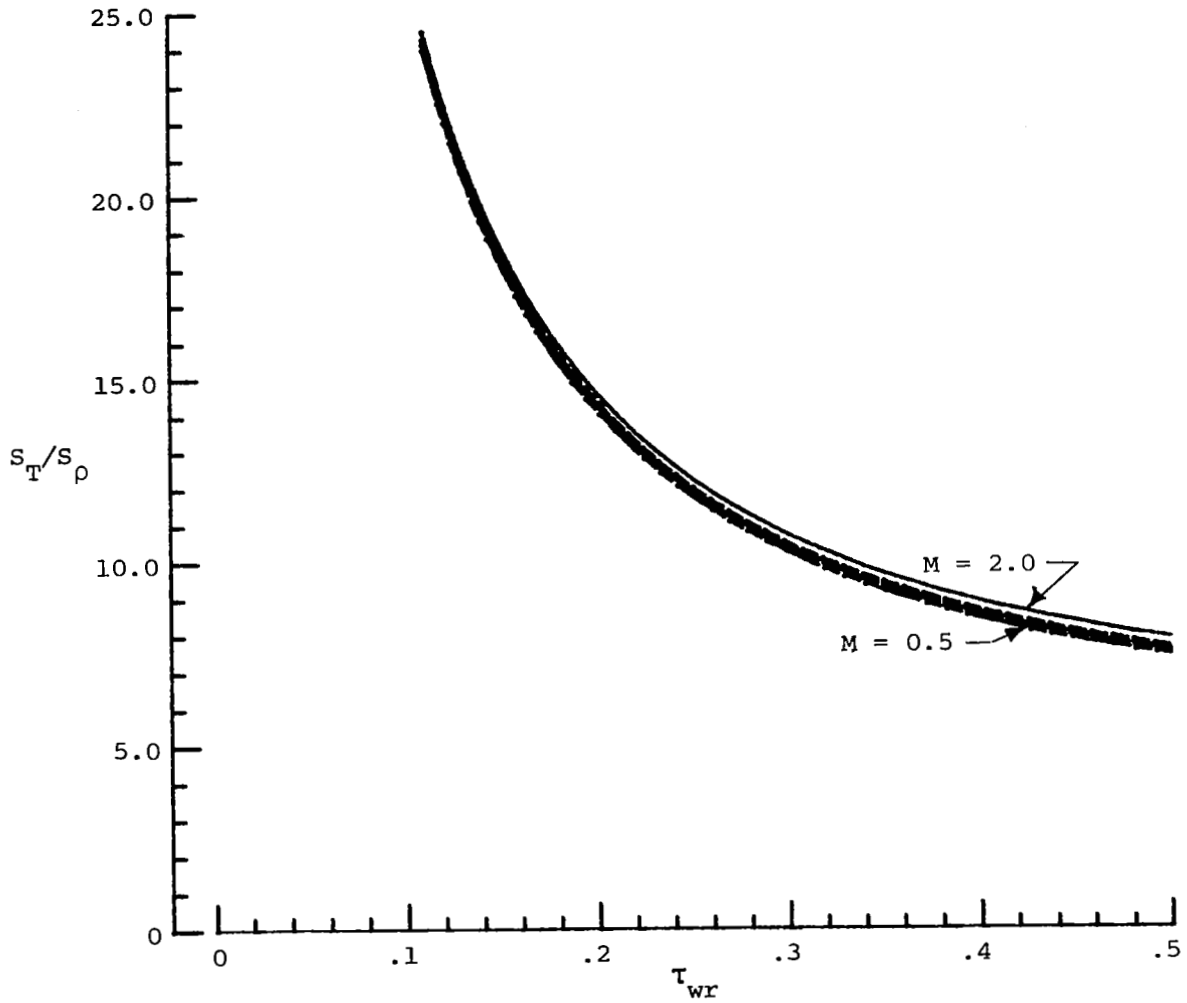

(a) Mach number as parameter. Re_∞ = 35000.

Figure 19.- Estimated variation of temperature-to-density sensitivity ratio with temperature loading.

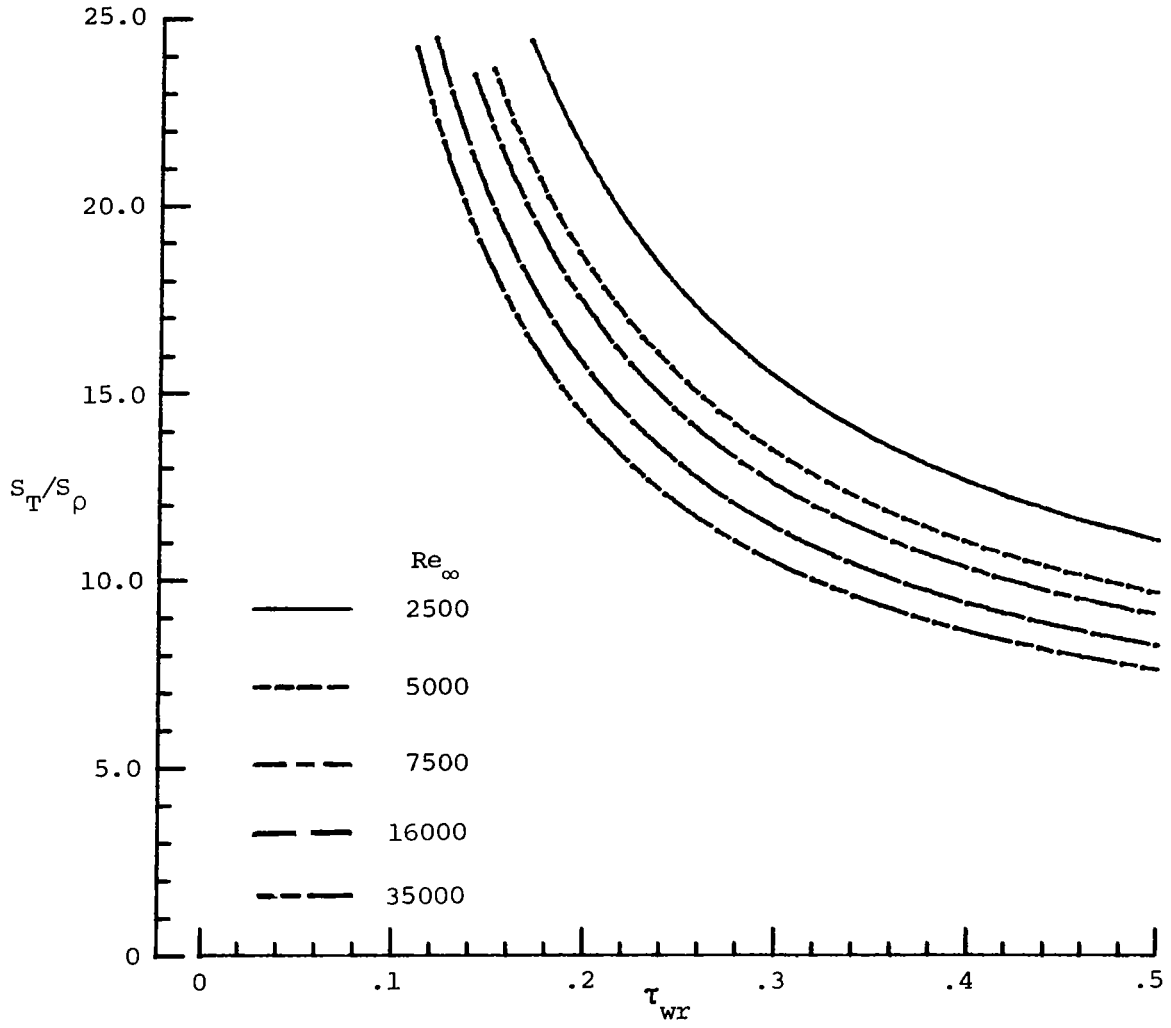

(b) Free-stream Reynolds number as parameter. M = 1.25.

Figure 19.- Concluded.

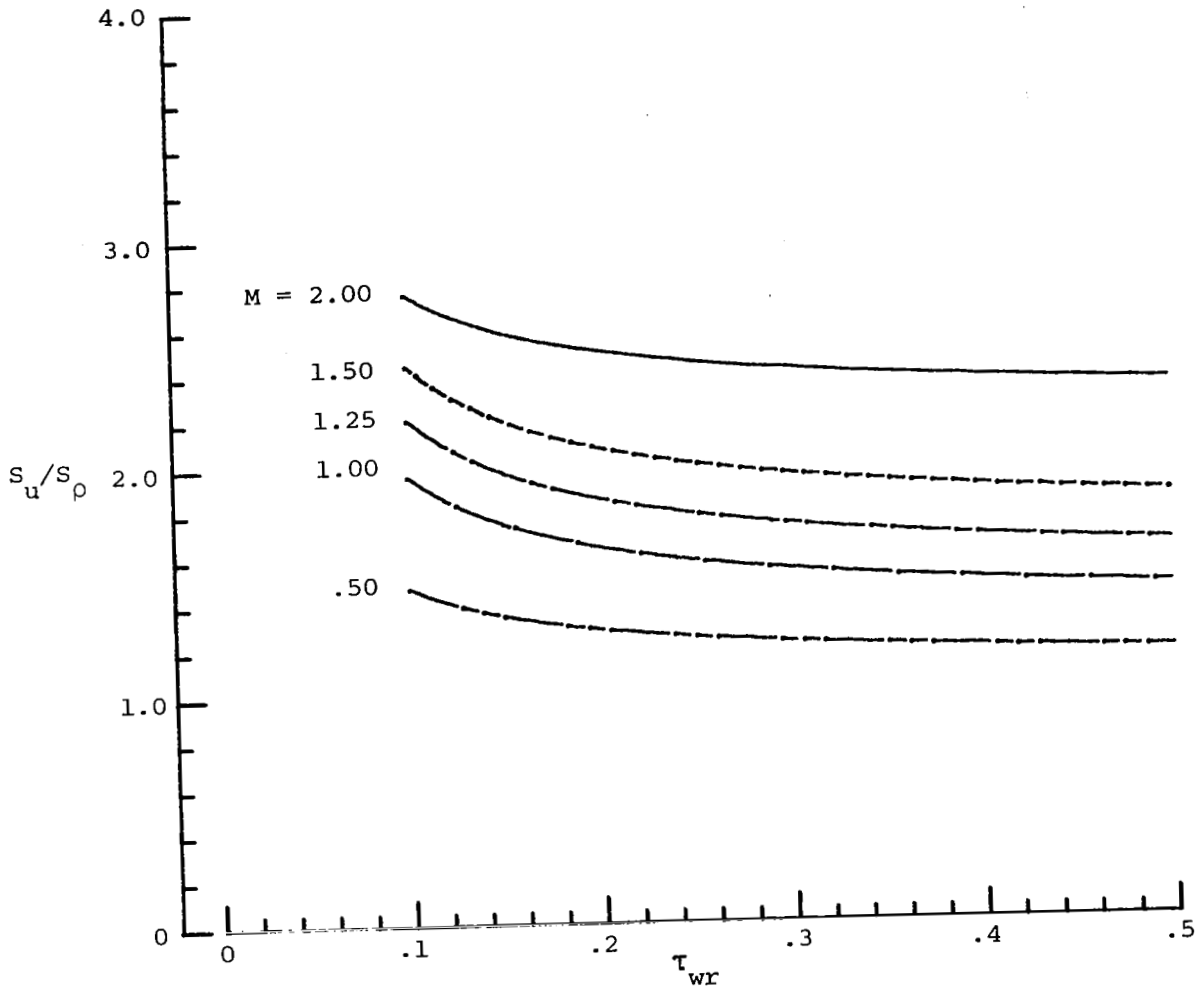

(a) $Re_\infty = 2500.$

Figure 20.- Estimated variation of velocity-to-density sensitivity ratio with temperature loading.

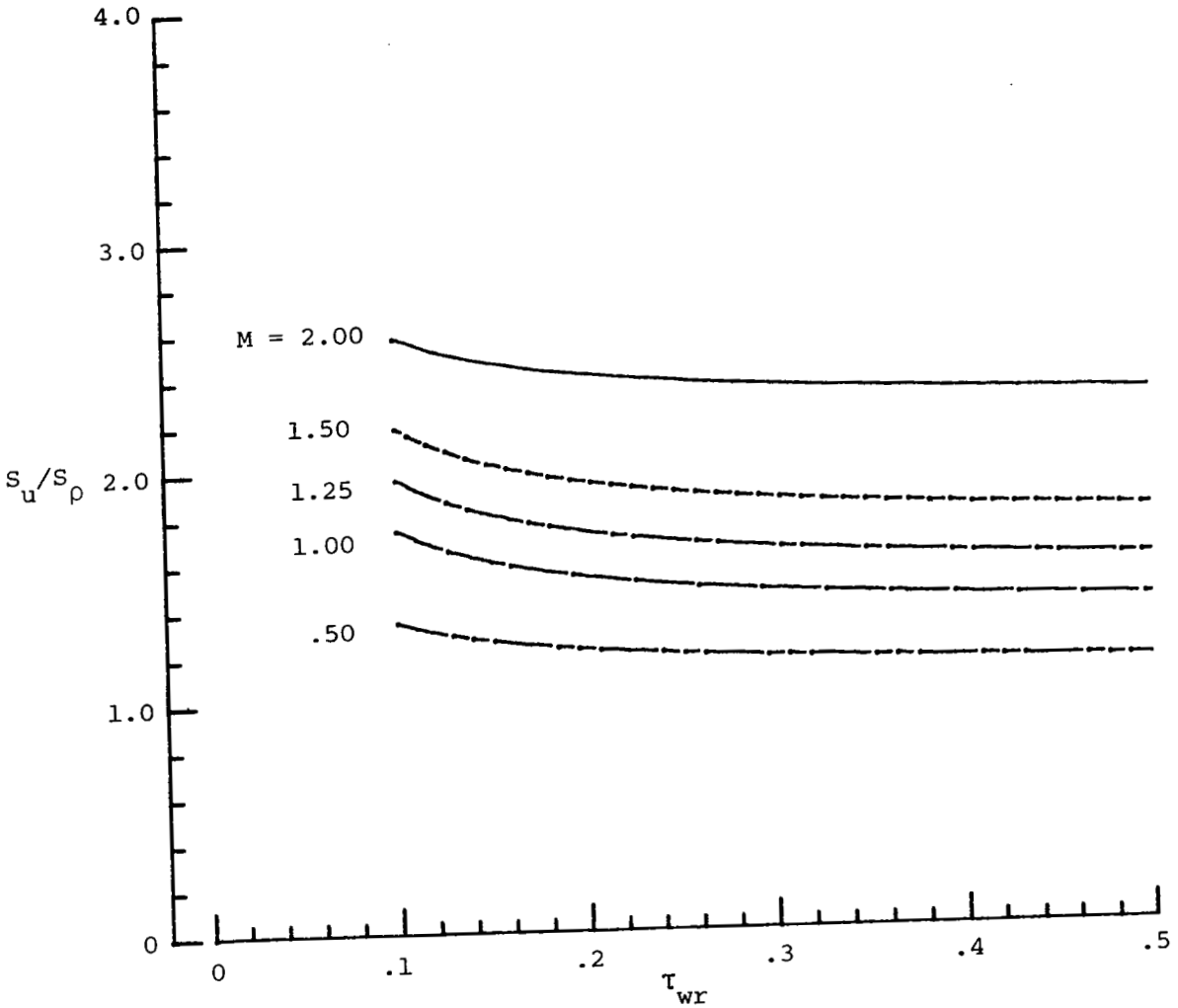

(b) $Re_\infty = 35000.$

Figure 20.- Concluded.

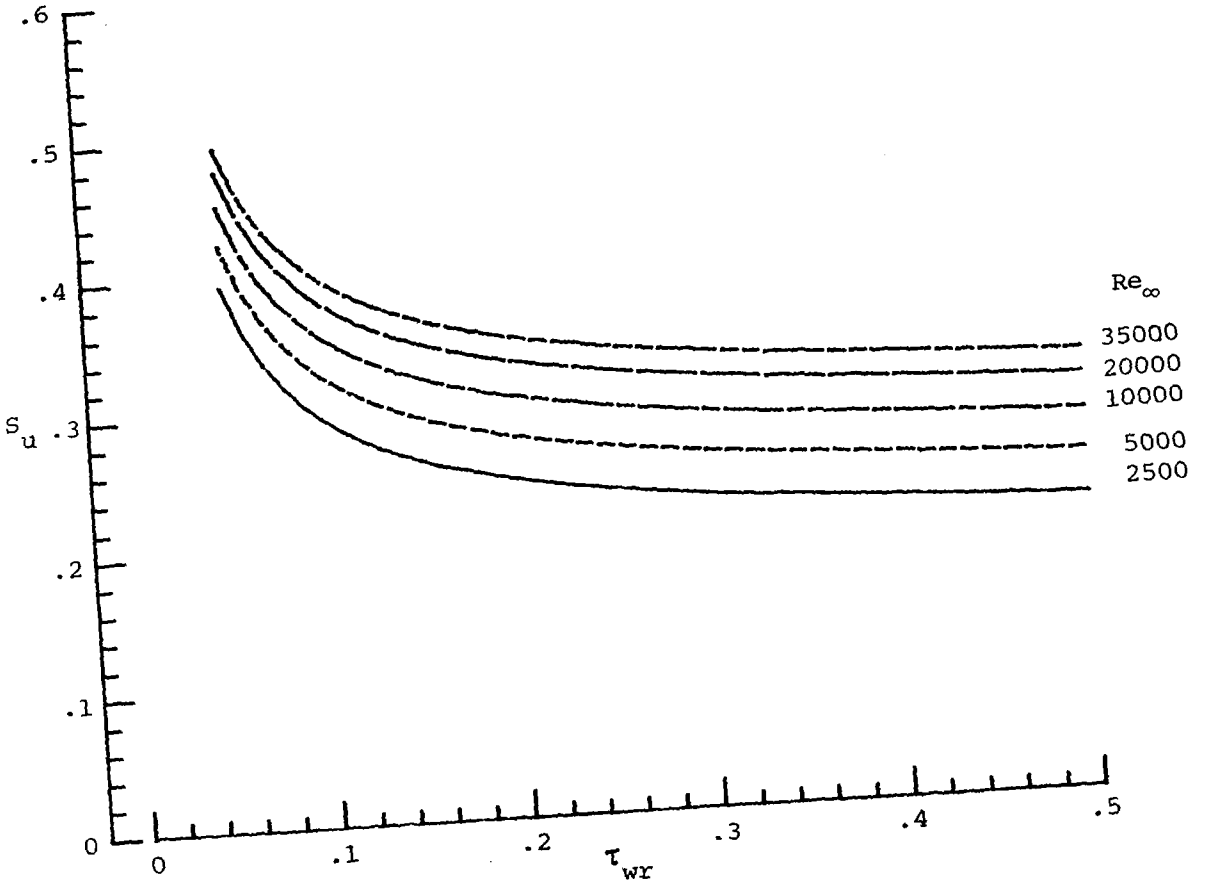

(a) Velocity sensitivity.

Figure 21.- Estimated velocity and density sensitivity variations with temperature loading. M = 1.25.

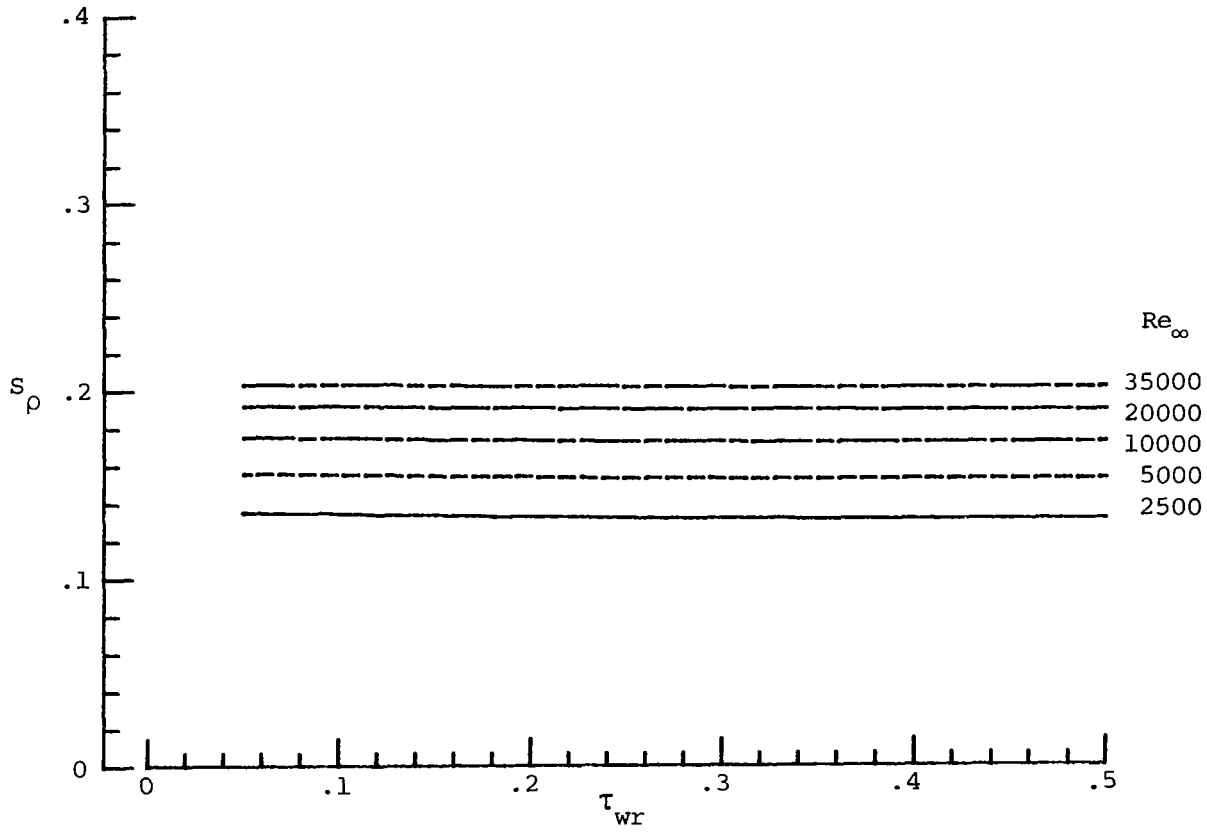

(b) Density sensitivity.

Figure 21.- Concluded.

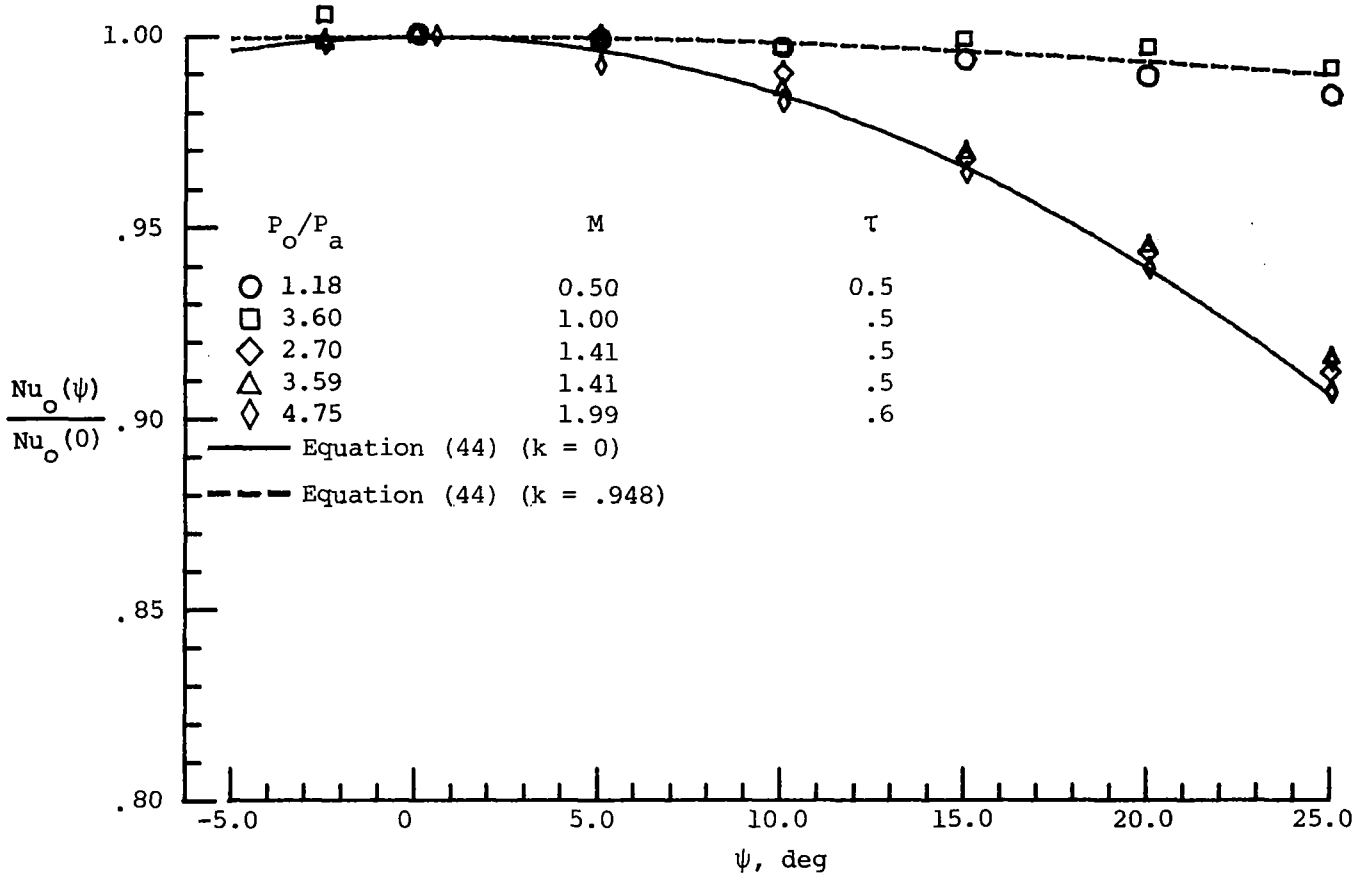

Figure 22.- Directional yaw response of cylindrical hot-film probe 3 at various Mach numbers.

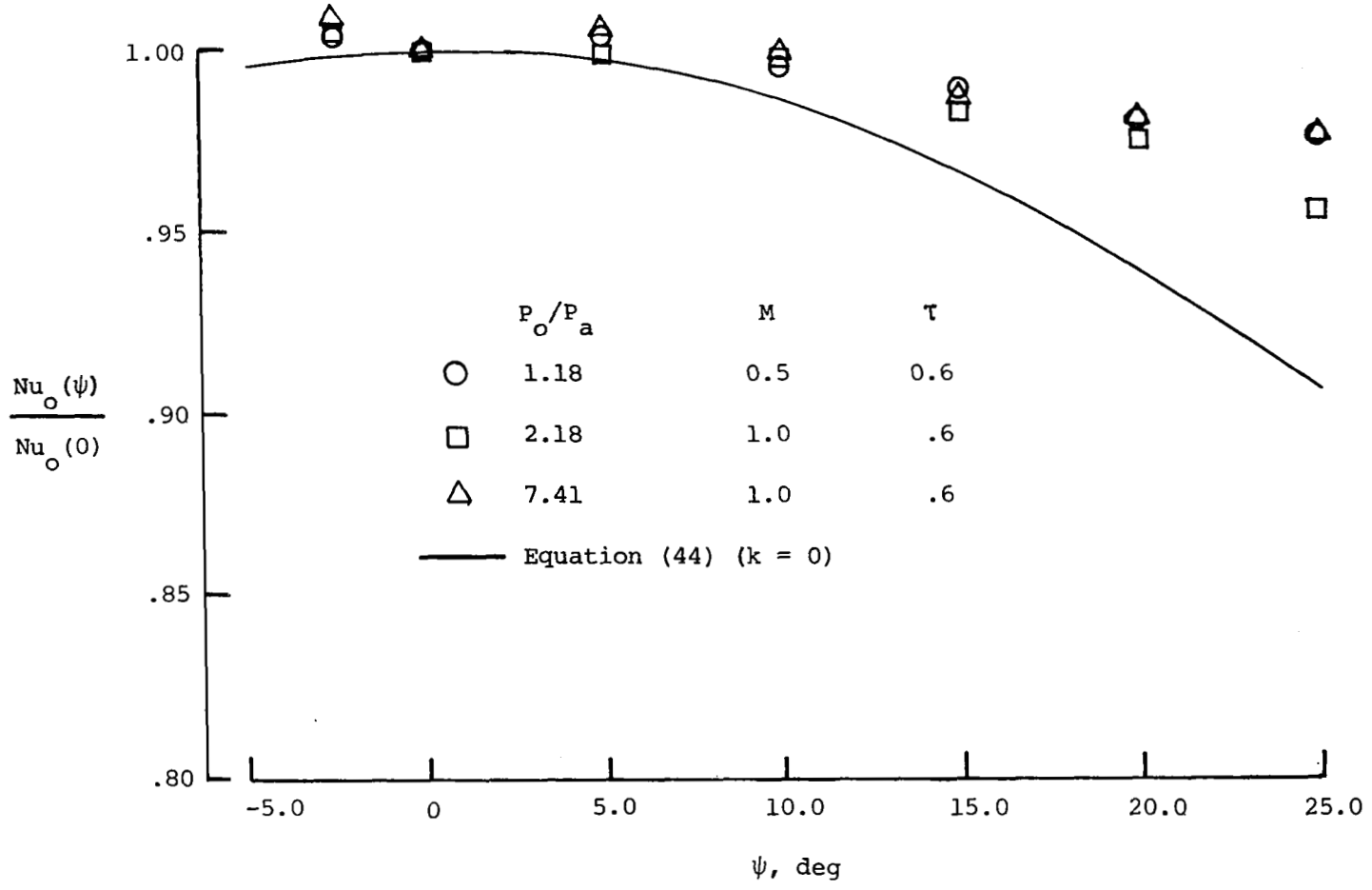

Figure 23.- Directional yaw response of wedge hot-film probe Y at subsonic and sonic speeds.

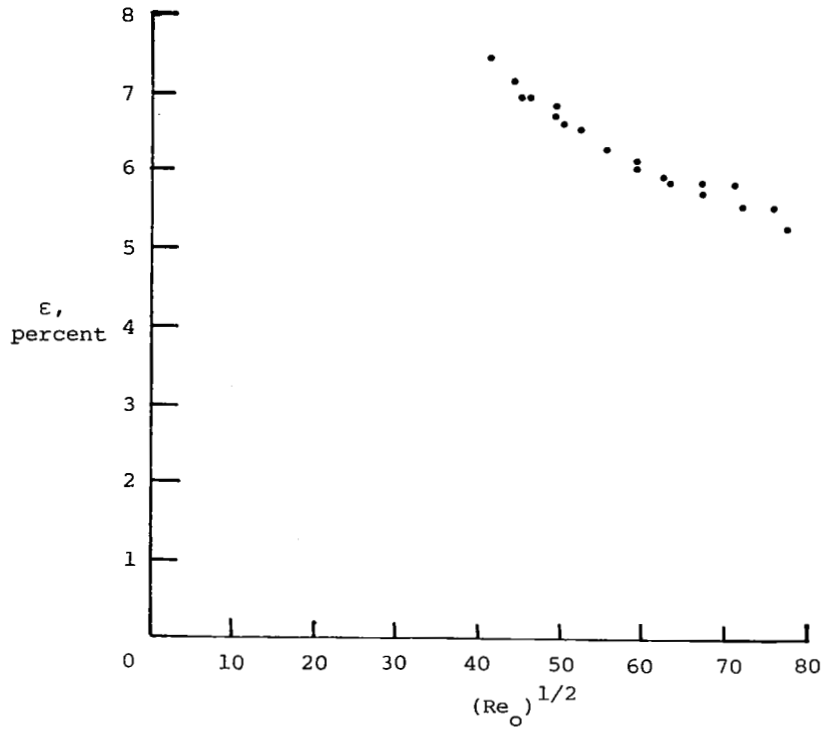

(a) $\tau = 0.25$.

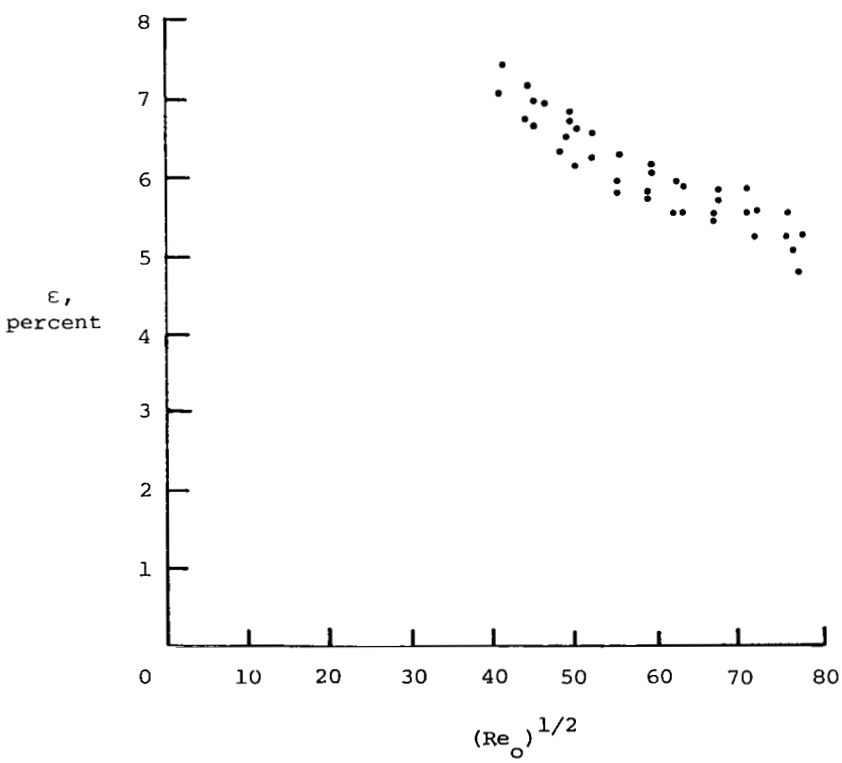

(b) $\tau = 0.5$.

Figure 24.- Estimate of conduction end loss for all Mach numbers.

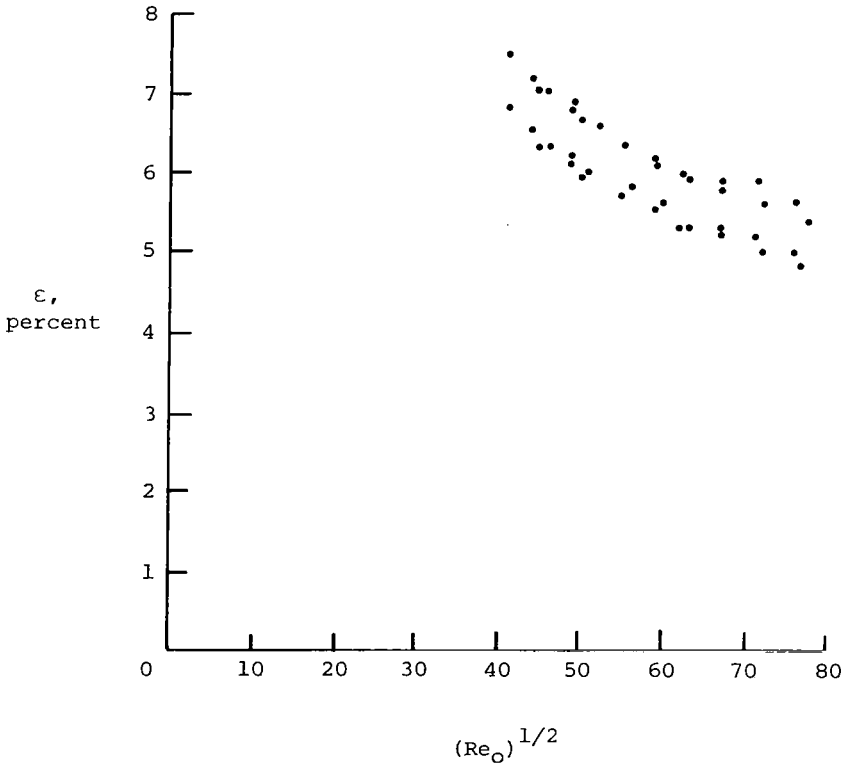

(c) $\tau = 0.75$.

Figure 24.- Concluded.

1. Report No.	2. Government Accession No.	3. Recipient's Catalog No.
NASA TP-2134		

4. Title and Subtitle	5. Report Date
THE WEDGE HOT-FILM ANEMOMETER IN SUPERSONIC FLOW	May 1983
	6. Performing Organization Code: 505-32-03-05
7. Author(s): John M. Seiner	8. Performing Organization Report No.: L-15538
	10. Work Unit No.
9. Performing Organization Name and Address: NASA Langley Research Center, Hampton, VA 23665	11. Contract or Grant No.
	13. Type of Report and Period Covered: Technical Paper
12. Sponsoring Agency Name and Address: National Aeronautics and Space Administration, Washington, DC 20546	14. Sponsoring Agency Code

15. Supplementary Notes

16. Abstract

A commercial wedge hot-film probe is studied to determine its heat transfer response in transonic to low supersonic flows of high unit Reynolds number. The results of this study show that its response in this flow regime differs from the response of cylindrical type sensors. Whereas the cylindrical sensor has the same sensitivity to velocity as to density for free-stream Mach numbers exceeding 1.3, the wedge probe sensitivity to velocity is always greater than its sensitivity to density over the entire flow regime. This property requires determination of three fluctuation components - due to density, velocity, and temperature - in a transonic or supersonic turbulent flow. Sensitivity equations are derived based on the observed behavior of the wedge probe. Both the durability and the frequency response of the probe are excellent, the square wave insertion test indicating frequency response near 130 kHz. The directional response of the probe at sonic speed is poor and requires further examination before Reynolds stress measurements are attempted with dual sensor probes.

17. Key Words (Suggested by Author(s))	18. Distribution Statement
Supersonic Turbulence Anemometry	Unclassified - Unlimited Subject Category 71

19. Security Classif. (of this report)	20. Security Classif. (of this page)	21. No. of Pages	22. Price
Unclassified	Unclassified	56	A04

For sale by the National Technical Information Service, Springfield, Virginia 22161

NASA-Langley, 1983